ANALYSIS OF SYSTEM SIGNALS BASED ON CROSS RECURRENCE METHOD FOR SYSTEM DYNAMICS CHARACTERIZATION

A Thesis

submitted in partial fulfillment of the degree of

DOCTOR OF PHILOSOPHY

by

JACOB ELIAS

KOCHI-682 022

**DIVISION OF MECHANICAL ENGINEERING,
SCHOOL OF ENGINEERING COCHIN UNIVERSITY OF SCIENCE AND TECHNOLOGY,
KERALA, INDIA**

NOVEMBER - 2011

DEDICATED TO MY PARENTS

DECLARATION

I hereby declare that the work presented in this thesis entitled "Analysis of System Signals Based on Cross Recurrence Method for System Dynamics Characterization" is based on the original work done by me under the supervision and guidance of Dr. Narayanan Namboothiri V.N., Faculty Division Of Mechanical Engineering, School of Engineering, Cochin University of Science and Technology. No part of this thesis has been presented for any other degree from any other institution.

Thrikkakara Jacob Elias

3-11-2011

CERTIFICATE

This is to certify that the thesis entitled "Analysis of System Signals Based on Cross Recurrence Method for System Dynamics Characterization" is a report of the original work done by Sri. Jacob Elias under my supervision and guidance in the School of Engineering, Cochin University of Science and Technology. No part of this thesis has been presented for any other degree from any other institution.

Thrikkakara
3-11-2011

Dr. Narayanan Namboothiri V.N.
Supervising Guide,
Division of Mechanical Engineering,
School of Engineering
Cochin University of Science and Technology, Kochi

Acknowledgements

I have proud privilege in recording my deep sense of gratitude to Dr. Narayanan Namboothiri V.N., my supervising guide and HOD of the Division of Mechanical Engineering, School of Engineering, CUSAT for suggesting this problem and for his invaluable guidance and encouragement throughout the course of my research. Working with him has been a great experience and I am indebted to him for his valuable support and fruitful discussions extended at all stages of this work.

I would like to thank Dr. David Peter S, Principal, School of Engineering, Cochin University of Science and Technology for providing me the resources and facilities to carry out this work.

I express my profound gratitude to Dr. P.S. Sreejith, former Principal and HOD of the Division of Mechanical Engineering, School of Engineering, Cochin University of Science and Technology, for all the help provided.

Thanks are due to members of the Research Committee of School of Engineering, for their kind suggestions at various stages of this work.

I am indebted to Prof. V.P. Narayanan Nampoori, an eminent personality with vast experience and profound insight from the International School of Photonics for his inspiration and support during this tenure.

I would like to gratefully acknowledge the stimulating discussions and timely advice from Prof. Charles L. Webber, Jr., Loyola University Chicago, and Dr. Norbert Marwan, Potsdam Institute for Climate Impact Research, Potsdam, Germany, at various stages of this work; they have enriched the work with new ideas and suggestions.

I am thankful to Dr. Rajesh V.G. and Dr Shouri P. S., faculty , Model Engineering College , Thrikkakara, for the assistance at various stages and also for help rendered for conducting elaborate tests required for this work.

Let me express my sincere gratitude to Dr. Usha Nair and Dr. Bindu M Krishna for their support during the course of my work. I am indebted to them for their whole hearted co-operation. Thanks are due to Sri Babu Varghese of the Machine Shop for his great help in setting up and performing the experiments in the machine shop. I would like to acknowledge Dr. Radhakrishnan P.M., Sri. Anslam Raj, Sri. Bijesh Paul and Sri. Jose Jacob for their timely help in completing this work. Let me also thank Sri. Jobin and Sri. Bibin for their technical assistances in the setup of the sensors.

I sincerely thank all my friends and colleagues in School of Engineering where I am working for their support and co-operation.

Thanks are also due to Yadu Krishnan and Yadhu Krishnan, students, International School of Photonics for their valuable assistance in setting up and conducting the experiments.

I thank the members of my family, Thara for her endless and manifold support and encouragement; my daughter Meera and son Manu for their patience with me.

Finally I thank God almighty for His mercy and blessings, without which this work would not have materialised.

ABSTRACT

Natural systems are inherently non linear. Recurrent behaviours are typical of natural systems. Recurrence is a fundamental property of non linear dynamical systems which can be exploited to characterize the system behaviour effectively. Cross recurrence based analysis of sensor signals from non linear dynamical system is presented in this thesis. The mutual dependency among relatively independent components of a system is referred as coupling. The analysis is done for a mechanically coupled system specifically designed for conducting experiment. Further, cross recurrence method is extended to the actual machining process in a lathe to characterize the chatter during turning. The result is verified by permutation entropy method.

Conventional linear methods or models are incapable of capturing the critical and strange behaviours associated with the dynamical process. Hence any effective feature extraction methodologies should invariably gather information thorough nonlinear time series analysis. The sensor signals from the dynamical system normally contain noise and non stationarity. In an effort to get over these two issues to the maximum possible extent, this work adopts the cross recurrence quantification analysis (CRQA) methodology since it is found to be robust against noise and stationarity in the signals.

Two sensor signals from a coupled system are recorded simultaneously at the same frequency. A cross recurrence plot enables the study of synchronisation or time differences in two time series. By conducting a cross recurrence quantification analysis, the behaviour of the coupled system can be studied. Subtle nonlinear behaviours of fluid-coupled mechanical oscillators at low and medium viscosities are better detected by cross recurrence analysis. Cross recurrence with its high sensitivity to nonlinear dynamics has applicability to weakly coupled oscillators also.

Metal cutting is a complex nonlinear dynamical process. The self-excited vibration caused by the regenerative effect, usually called chatter, is created during machining when any one of the cutting parameters increases above a critical value. Cross recurrence plot based methodology is used to find the point of transition from normal cutting to chatter cutting. In this method two signals - one input signal (power to the lathe motor) and one output signal (cutting tool vibration) - are recorded simultaneously at a constant sampling rate during cutting. These two different time series are used to create cross recurrence plot (CRP). This CRP can be quantified using CRQA. Abrupt variation in the CRQA parameters indicates the onset of chatter.

The study reveals that the CRQA is capable of characterizing even weak coupling among system signals. It also divulges the dependence of certain CRQA variables like percent determinism, percent recurrence and entropy to chatter unambiguously. The surrogate data test shows that the results obtained by CRQA are the true properties of the temporal evolution of the dynamics and contain a degree of deterministic structure.

The results are verified using permutation entropy (PE) to detect the onset of chatter from the time series. The present study ascertains that this CRP based methodology is capable of recognizing the transition from regular cutting to the chatter cutting irrespective of the machining parameters or work piece material. The results establish this methodology to be feasible for detection of chatter in metal cutting operation in a lathe.

Table of contents

List of Tables

List of Figures

Abbreviations

%DET	Percent Determinism
%LAM	Percent Laminarity
%REC	Percent Recurrence
AMI	Average Mutual Information
CER	Coarse-grained Entropy Rate
CRP	Cross Recurrence Plot
CRQA	Cross Recurrence Quantification Analysis
CT	current transformer
DM	Distance Matrix
DIV	divergence
EIB	encoder interfacing box
ENT	Entropy
FNN	False Nearest Neighbour
LMAX	Linemax
LOI	Line of Identity
LOS	line of synchronization
NTSA	Nonlinear Time Series Analysis
RM	Recurrence Matrix
RP	Recurrence Plot
RPs	Recurrence Plots
RQA	Recurrence Quantification Analysis
RR	Recurrence Rate
TT	Trapping Time

1. Introduction

Physical systems exhibit highly nonlinear, chaotic, and unpredictable behaviour. Linear analysis of these processes does not capture several critical and strange behaviours encountered in the real world situations. Characterisation of signals of non linear dynamical systems and the extraction of useful information provide significant insight into the type of behaviour shown by the system. Analysis of real world phenomena using methods of non linear dynamics is based on the state space to describe the state and behaviour of the system. Machining process is one of the areas in which nonlinear approach with fast and robust technique of characterisation monitoring and control is essential. This thesis focuses on the study of dynamics of the coupled system, especially machining chatter by the method of Cross Recurrence Quantification Analysis (CRQA) to bring out the dynamics of the system.

Machining is one of the most common operations in a manufacturing system. Most of the products manufactured all over the world undergo a machining process at some stage of their production. A sizable fraction of the value of the manufactured products is the cost of machining. Good machinability is an optimal combination of

factors such as low cutting force, good surface finish, low tool tip temperature and low power consumption. In the manufacturing process, there are two main practical problems that engineers face. The first is to determine the process parameters that will yield the desired product quality and the second is to maximize manufacturing system performance using the available resources.

In every machining process, the choice of optimal cutting parameters such as speed, feed and depth of cut is of vital importance. Optimization of machining parameters not only increases the utility for machining economics, but also enhance the product quality to a great extent. The most widely used index of product quality is surface roughness. In many cases, it is a technical requirement for mechanical products. The functional behaviour of a part depends on obtaining the desired surface quality. The process dependent nature of the surface roughness formation mechanism along with the numerous uncontrollable factors makes it almost impossible to get a direct solution.

Chatter during machining, manifested as the undulating pattern of marks in a machined surface from the vibration of the tool or workpiece, correspond to the relative movement between the work piece and the cutting tool. The vibrations result in waves on the machined surface. This affects typical machining processes, such as turning, milling and drilling, and atypical machining processes, such as grinding. Chatter results in poor surface quality, unacceptable inaccuracy, excessive

noise, tool wear, machine tool damage, reduced metal removal rate waste of materials and waste of energy.

Modelling based on chaos theory has led to the finding that metal cutting exhibits low dimensional chaos under normal operating conditions. A mechanical system signal is by nature non-stationary and is usually corrupted with dynamic or measurement noise which necessitates pre-processing. Signal analysis of such a data, therefore, requires an analysis methodology that is tested to be robust against these two important attributes. Moreover, most methods of nonlinear data analysis methodologies need rather long data series.

Recently new methods based on nonlinear data analysis have become popular particularly Recurrence Plots (RPs) and Cross Recurrence plots (CRPs). Recurrence is a fundamental property of dissipative dynamical systems. Although small disturbances of such a system cause exponential divergence of its state, after sometime the system will come back to a state that is arbitrarily close to a former state and pass through a small evolution. RPs and CRPs visualize such recurrent behaviour of dynamical systems. Practitioners of these methods have found its relevance for short, noisy and non-stationary data. These features are indeed the crucial advantage. Deduction of information by visually examining the RPs and CRPs is more subjective. Hence it is developed into Recurrence Quantification Analysis (RQA) and Cross Recurrence Quantification Analysis (CRQA). This quantifies the number and duration of recurrences of a dynamical system presented by its phase space trajectory. The Features extracted from the CRPs by CRQA, contain

information about the system. These features are called CRQA variables and can be used for characterizing a dynamical system.

Since the CRQA methodology is found to provide useful information even for short, non-stationary and noisy data; this analytical tool can be ideally suited for the characterization of complexity in a mechanical system exhibiting chaotic behaviour. The present work, therefore, adopts the CRQA methodology for the analysis of sensor signals captured from a coupled system. After ascertaining the suitability of CRQA method for the system signals from coupled system, it is used in the analysis of a real world problem of machining chatter. The work attempts to characterize the system signals generated, first by identifying the significant CRQA variables, and then by studying their sensitivity to chatter.

1.1 Motivation

Many of the existing signal analysis methods fail or mislead in the presence of noise and non-stationarity. Most of the real time processes deal with huge data sets contaminated with dynamical and observational noise. Nonlinear time series analysis based on CRP methods addresses these issues in a more effective manner.

The CRQA can provide useful information even from a short data set, which makes it an attractive feature extraction methodology suitable for deployment in the monitoring of real-time cutting process.

1.2 Aim of the Thesis

This thesis aims at exploring the recurrent behaviour of the dynamical system. There is valuable information hidden in such behaviour of the system. To make use of a versatile signal processing methodology called CRQA to emphasize and extract the information contained in machining dynamics is the primary aim of the study. Sensor signal characteristics have been given an important role throughout the work. More specifically, the aim of this thesis is to:

- To study the nonlinear characteristics of a coupled system.
- To investigate the applications of CRP-based approaches in characterizing the dynamics of coupled systems
- To study and experimentally validate the applicability of CRQA methodology in detecting chatter in turning.

1.2 Thesis Outline

Chapter 1 introduces the problem and defines the aim of the thesis

Chapter 2 contains a review of background literature on coupled systems, machine chatter, nonlinear time series analysis methods, dynamics of cutting process and CRP based approaches in the context of signal processing.

Chapter 3 portrays the experimental frame work and research methodology adopted in the thesis.

Chapter 4 deals with the experimental setup and the data acquisition systems used in the coupled oscillator experiments. The analysis of the result of the experiments is also done.

Chapter 5 presents the experimental setup and the data acquisition systems used in the machining experiments. This also renders the experimental results and analysis of the results.

Chapter 6 presents conclusions with pointers for future work.

2. Background Literature Review

This chapter gives the background for up-coming sections. It is an assessment of the present state of the wide and complex fields of coupling and machine tool chatter. Also, this chapter reviews what has been done in the past in the area of nonlinear dynamics of metal cutting process.

2.1 Coupled Systems

A dynamical system is one whose evolution is determined by its current state and past history. The system may be as simple as a swinging pendulum or as complicated as a turbulent fluid. In 1665 Christian Huygens [3] discovered that pendulum clocks mounted on a common wall would eventually swing in synchrony. This observation leads to the study of mutual dependency among relatively independent components which is referred as coupling. Coupling between signals is quantified by conventional methods such as relative phase relations, coherence analysis, or cross-correlation. However, these tools are linear and assume that individual components have additive mutual influences, rather than nonlinear multiplicative interactions. Many natural systems, physical and biological, are nonlinear, nonstationary and noisy, and thereby violate many of the assumptions of traditional linear methods.

Hedrih [1] has conducted a survey in the area of dynamics of coupled rotations and coupled systems. Also, a survey of models and dynamics of coupled systems composed of a number of deformable bodies (plates, beams or belts) with different properties of materials and discrete layer properties is done. The constitutive stress–strain relations for materials of the coupled sandwich structure elements are described for different properties: elastic, viscoelastic and creeping. The characteristic modes of the coupled system vibrations are obtained and analyzed for different kinds of materials and structure composition. Structural analysis of sandwich structure vibrations is done. The author had concluded that coupled rigid and simple nonlinear subsystems in the nonlinear dynamics of the resultant system dynamics introduce hybrid complex nonlinear dynamics with multiplications of the singularity phenomenon.

Pogromsky and Nijmeijer [2] made a qualitative study of the dynamics of a network of diffusively coupled identical systems. In particular, they derived conditions on the systems and on the coupling strength between the systems that guarantee the global synchronization of the systems.

Shockley et al. [3] studied about the coupled oscillators and they have described Recurrence quantification analysis (RQA) which was originally designed by Webber and Zbilut [4,5] to study the recurrent structuring of single signals that were time delayed and embedded in higher dimensional space. These auto recurrence plots were demonstrated to have utility in diagnosing the states of a variety of

dynamical systems [6]. Cross recurrence quantification analysis (CRQA) was introduced by the same authors [7] to examine the intricate recurrent structuring between paired signals which were also time-delayed and embedded in higher dimensional space.

In this paper [3] the driver oscillator was a sine wave generator but the motions of the coupled rotor oscillator were much more complex and delicate (nonlinear). CRQ method was able to take out non-obvious dynamic characteristics of the weak couplings not assailable by spectral analysis or return maps.

Pecora and Carroll [8] showed that many coupled oscillator array configurations considered can be put into a simple form so that determining the stability of the synchronous state can be done by a master stability function, which can be tailored to one's choice of stability requirement. This solves the problem of synchronous stability for any linear coupling of that oscillator.

Ito et al. [9] studied about the circularly coupled oscillator system that consist of many locally connected subsystems, especially oscillators, that produce linear state relations. The relations are defined between two connected subsystems, where their references are also assigned as a goal behaviour simultaneously. A mathematical description of the subsystem interactions are clarified by extending a method based on the gradient dynamics. As an example of this formulation, the relative phase control of the circularly coupled oscillator system is considered, where the oscillation with the uniform phase lag should be achieved. This oscillator system

is applied to the timing controller for the multicylinder engine. It is clarified that monotonically increasing odd functions are available to describe the effect from the connected subsystems. Making the definition of the subsystem interactions clear, a rule of references adjustment was proposed so as to reduce these interactions. In addition, the reference of the relative phase was adjusted to an appropriate and achievable one in the prevailing conditions.

Ren et al. [10] studied the relationship between dynamical properties and interaction patterns in complex coupled oscillator networks in the presence of noise. They found that noise leads to a general, one-to-one correspondence between the dynamical correlation and the connections among oscillators for a variety of node dynamics and network structures. The universal finding enables an accurate prediction of the full network topology based solely on measuring the dynamical correlation. There is a high success rate in identifying links for distinct dynamics on both model and real-life networks. This method can have potential applications in various fields due to its generality, high accuracy and efficiency.

Odibat [11] wrote a note on phase synchronization in coupled chaotic fractional order systems. The control and reliable phase synchronization problem between two coupled chaotic fractional order systems is addressed in this paper. An active nonlinear feedback control scheme is constructed to achieve phase synchronization between two coupled chaotic fractional order systems. The necessary conditions for fractional order Lorenz, Lü and Rössler systems to exhibit chaotic attractor similar to their integer order counterpart. Then, based on the stability results of fractional

order systems, sufficient conditions for phase synchronization of the fractional models of Lorenz, Lü and Rössler systems are derived. The synchronization scheme enables synchronization of fractional order chaotic systems to be achieved without the computation of the conditional Lyapunov exponents. Numerical simulations are performed to assess the performance of the analysis.

There are many methods of analysing the coupled oscillator problem. In real life also many instances of coupling are encountered. Machining is one of them. When one of the cutting parameters increase beyond a level, chattering may occur, which is detrimental for the machining.

2.2 Chatter Research

Metal cutting processes can involve three different types of mechanical vibrations that arise due to the lack of dynamic stiffness of one or several elements of the system composed by the machine tool, the tool holder, the cutting tool and the workpiece material. These three types of vibrations are known as free vibrations, forced vibrations and self-excited vibrations [12]. Free vibrations occur when the mechanical system is displaced from its equilibrium and is allowed to vibrate freely. In a metal removal operation, free vibrations appear, for example, as a result of an incorrect tool path definition that leads to a collision between the cutting tool and the workpiece. Forced vibrations appear due to external harmonic excitations. The principal source of forced vibrations in milling processes is when the cutting edge enters and exits the workpiece. However, forced vibrations are also associated, for example, with unbalanced bearings or cutting tools, or it can be transmitted by other

machine tools through the workshop floor. Free and forced vibrations can be avoided, reduced or eliminated when the cause of the vibration is identified. Engineers have developed several widely known methods to mitigate and reduce their occurrence. Self-excited vibrations extract energy to start and grow from the interaction between the cutting tool and the workpiece during the machining process. This type of vibration brings the system to instability and is the most undesirable and the least controllable. For this reason, chatter has been a popular topic for academic and industrial research.

The search for reasons of machine tool vibrations and instabilities appeared at the beginning of the 20th century. This is a result of vast improvement in metal removal process. In the last century machine tools witnessed a considerable evolution and became more powerful, precise, rigid and automatic. This growth was fuelled by general industry development, especially in the case of aerospace, moulding and automotive industries. But with all these improvements in the manufacturing sector, new limitations and challenges also appeared. Machines and structures are not rigid bodies, but rather systems consisting of elastic components that respond to external or internal forces with finite deformations. In addition, there are relative motions between the components, giving rise to internal forces. Due to these internal and external forces, the machine or structure moves. This motion, as a result of internal and external forces, is the subject of dynamics and vibration [13]. In 1907, Taylor [14] stated that chatter is the ‘‘most obscure and delicate of all problems facing the machinist’’. Many years later, Tobias [12] wrote: ‘‘Machine tool development in

recent decades has created an increasing number of vibration problems. Machine tool designers in early development phases are worried about vibration characteristics; production engineers know that vibrations diminish tool life, generate unacceptable surface finishes on the parts and reduce productivity''. Vibrations are still considered as a limiting factor, one of the most important machining challenges and, an aspect to be improved.

Chatter is generally classified in two categories: primary and secondary. Primary chatter is caused by the cutting process itself (i.e. by friction between the tool and the workpiece, by thermo-mechanical effects on the chip formation or by mode coupling). Secondary chatter may be caused by the regeneration of waviness of the workpiece surface. This regenerative effect is the most important cause of chatter. It is possible to distinguish between frictional chatter, thermo-mechanical chatter and mode coupling chatter and regenerative chatter depending on the self-excitation mechanism that causes the vibration.

The most common approach to chatter detection is to investigate the spectral density of a process signal and develop a threshold value that indicates chatter. Delio et al.[15] and Altintas and Chan [16] investigated sound pressure as the process signal. Tarng and Li [17] created threshold values for the spectrum and the standard deviation of thrust forces and torque signals in machining operations

Clancy and Shin [18] presents a three-dimensional mechanistic frequency domain chatter model for face turning processes, that can account for the effects of tool

wear including process damping. New formulations are presented to model the variation in process damping forces along nonlinear tool geometries such as the nose radius. The model can be used to determine stability boundaries under various cutting conditions and different states of flank wear. Chatter was identified by two methods: by verifying the spectrum of the acceleration signals, and by measuring the resultant surface roughness. A large spike in the spectrum close to the natural frequency of the system is a good indicator of chatter. As chatter occurs the tool vibrates violently and thus creates an undulated pattern on the workpiece. This creates a rougher surface than those in stable cutting, and hence surface roughness is also a good indication of chatter occurrence. An improved three-dimensional frequency domain chatter prediction model is developed, which accounts for the effects of tool wear This model can be used with complex geometry tools to accurately predict the magnitude and direction of the process damping force.

Grabec, Gradisek and Govekar [19] developed a new method for detection of chatter onset based on characterization of changes in process dynamics. It is demonstrated by the experiments with turning in which the transition to chatter is caused by variation of cutting depth. The signal of cutting force is characterized by the normalized coarse grained entropy rate whose value exhibits a drastic drop at the onset of chatter. For the purpose of automatic on-line chatter detection a characteristic value of coarse-grained entropy rate (CER) is determined which is rather insensitive to variation of cutting conditions. Experiments with single point turning on a lathe were conducted with continuous changing of the cutting depth in

order to demonstrate the performance of a new method of chatter detection. Experiments show that CER is a robust, relative characteristic that can effectively be applied for on-line characterization of short and noisy time series obtained from a manufacturing processes in an industrial environment. A low CER value is typical for chatter. Their experiments show that the value of normalized CER below the level 0.2 reliably indicates chatter, regardless of cutting conditions and cut material.

Li, Wong and Nee [20] developed a technique to identify both tool wear and chatter in turning a nickel-based super alloys. The coherence function between two crossed accelerations from the bending vibration of the tool shank is used. The value of the coherence function at the chatter frequency reached unity at the onset of chatter. Its values at the first natural frequencies of the tool shank approached unity in the severe tool wear stage. The results are interpreted using the analysis of the coherence function for a single input-two output model.

Pratt and Nayfeh [21] had done chatter control and stability analysis of a cantilever boring bar under regenerative cutting conditions. Both theoretical and experimental investigations were done. The bar has been equipped with actuators and sensors for feedback control of its structural dynamics. It was modelled at the tool point by a mass spring damper system free to move in two mutually perpendicular directions. Their aim was to demonstrate the effect of simple feedback control on the parameter space of chatter-free machining in a boring process. Active control of the tool damping in each of the principal modal directions was implemented and shown

in theory and experiment to be quite effective at suppressing chatter. Problems caused by jumps from stable to unstable cutting due to nonlinear regenerative chatter effects are also considered. The case where the cutting forces are described by polynomial functions of the chip thickness was examined. They used a perturbation technique to calculate the nonlinear normal form of the governing equations to determine the post-linear instability (bifurcation) behaviour. This result was in qualitative agreement with experimental observations. An active control technique for changing the form of bifurcation from subcritical to supercritical was presented for a prototypical, single-degree-of-freedom model.

Xiao et al. [22] conducted experimental investigations to show that chatter is effectively suppressed without relying on the tool geometry by applying vibration cutting. In order to study the precision machining mechanism of vibration cutting, a new cutting model which contains a vibration cutting process is proposed by them. Simulations of the chatter model exhibit the main feature of chatter suppression in vibration cutting which are in agreement with the measurement values and accurately predict the work displacement amplitudes of vibration cutting. Experimental investigations show that chatter is effectively suppressed irrespective of the tool geometry by vibration cutting.

Litak [23] has analyzed Chaotic vibrations in a regenerative orthogonal turning process. The simple one degree of freedom model used includes the basic phenomena as friction between a chip and the tool, nonlinear power low character of the cutting force expression as well as the possibility of a contact loss between the

tool and the workpiece. The author could observe the complex behaviour of the system. In presence of a shaped cutting surface, the nonlinear interaction between the tool and a workpiece leads to chatter vibrations of periodic, quasi-periodic or chaotic type depending on system parameters. To describe the profile of the surface machined by the first pass he uses a harmonic function. He analyzed the impact phenomenon between the tool and a workpiece after their contact loss. It enables an intermittent transition from a regular to chaotic system behaviour.

Quintana and Ciurana [24] has done a review on chatter in machining processes. A great deal of research has been carried out since the late 1950s to solve the chatter problem. Researchers have studied how to detect, identify, avoid, prevent, reduce, control, or suppress chatter. They have classified the existing methods developed to ensure stable cutting into those that use the lobbing effect, out-of-process or in-process, and those that, passively or actively, modify the system behaviour. Due to the great variety of metal removal processes, machine tool structures, configurations and capabilities, tool holders, cutting tools and materials, etc., it is difficult to find a common solution for avoidance of chatter. Development of intelligent machines, able to perform auto-diagnosis in order to evaluate cutting process efficiency and make decisions for adapting the current cutting parameters to increase productivity while ensuring quality parameters can solve this problem.

Fansen, Peng and Xingang [25] developed a method for varying the spindle speed using chaotic signal to suppress chatter in machining. The effects of spindle speed variation on chatter control using chaotic and sinusoidal signals were analyzed by

simulation and experimental methods. Various chaotic codes are used in the chatter suppression process, and it is found that LORENZ-1 code results in the smallest machine noise. In time-varying speed machining, the beat vibration may happen if using periodic waves for speed variation. This beat problem can be overcome by using chaotic codes instead of periodic wave signals. Simulation shows that chatter suppression can be achieved by using chaotic codes, such as DUFFING, LORENZ-1, LORENZ-2, ROSSLER, and MACKEY-GLASS. However, the effectiveness is different, and LORENZ-1 was found to have the best performance in this study.

Many methods were developed to control chatter during machining. Still a lot of research is going on in this field. However it is seen that no work has been done to apply cross recurrence plot based methods to detect and thereby control chatter.

2.3 Cross recurrence plot

Recurrence plot is a method based on non linear data analysis. Eckman et al. [26] suggested the concept of Recurrence plot. They have concluded that it display important and easily interpretable information about time scales which are otherwise rather inaccessible.

Zbilut and Webber Jr. [27] extend the usefulness of this tool by quantifying certain features of these plots which are helpful in determining embeddings and delays. Schinkel, Dimigen, and Marwan [28] developed a method for choosing an appropriate threshold for the recurrence plot. The search for a recurrence threshold for an optimal discrimination of signals has revealed different optimal thresholds

depending on the application and considered type of signal. Using the recurrence probability alone for the detection require another threshold than using diagonal and vertical line structures. However, the differences in the optimal threshold are not big and the optimal threshold also depends on the amount of noise present in the measurement.

They proposed a new approach for the choice of an optimal recurrence threshold for the classification of signals which uses the notion of receiver operating characteristics, a statistical tool to validate a classification process and investigate its discriminative power in dependence of a given detector.

Kennel, Brown and Abarbanel [29] studied about determining an acceptable minimum embedding dimension by looking at the behaviour of near neighbours under changes in the embedding dimension from d to d+1. When the number of nearest neighbours arising through projection is zero in dimension d_E, the attractor has been unfolded in this dimension. The precise determination of d_E is clouded by noise. The authors examine the manner in which noise changes the determination of d_E. In an embedding dimension that is too small to unfold the attractor, not all points that lie close to one another will be neighbours because of the dynamics. Some will actually be far from each other and simply appear as neighbours because the geometric structure of the attractor has been projected down onto a smaller space. They use time-delay coordinates and attribute the disappearance of false neighbours as an indication of a minimum embedding dimension for the data. For this case the calculation that determines which is a near neighbour is performed in d dimensions,

while the calculation of the distance between neighbours is performed in (d+1) dimensions. The proportion of false neighbours is on an absolute scale, always bounded between 0 and 1.

Zbilut , Giuliani and Webber Jr. [30] studied about RQA and principal components in the detection of short complex signals. They demonstrated the utility of combining recurrence quantification analysis with principal components analysis to allow for a probabilistic evaluation for the presence of deterministic signals in relatively short data lengths.

There were many variables suggested to quantify RP's and have found effectiveness in different scientific explorations [31-40]. In particular, the following have been defined: the percentage of points that are recurrent (%REC – a global measure of recurrence); the percent of recurrent points which compose line segments and are therefore deterministic (%DET); the Shannon entropy of the histogram of varying line segment lengths as a rough measure of the information content of the trajectories (ENT); a measure of trajectory divergence derived from the length of the line segments which were claimed to be proportional to the inverse of the largest positive Liapunov exponent (DIV); a least squares regression from the diagonal to the plot's corner as a measure of stationarity insofar as a flat slope indicates strong stationarity, whereas large slopes indicate poor stationarity due to changing values from one portion of the plot to another, i.e., a paling of the graph (TREND) and mean

distance of the embedded points. All these variables provide information about various aspects of the plot, and were intercorrelated.

Zbilut et al. performed RQA on a time series of typical signal processing and chaotic data; in addition to randomly shuffled versions, and noise signals to provide examples of nonsignals. All data were 1000 points long, with an embedding of 10, a delay of 32, a Euclidean norm for distance calculations, a neighbourhood of 1 to define the recurrence, and line segments counted if composed of 2 or more points. The results reveal the utility by combining separate variables through principal components analysis (PCA) to provide a statistical estimation of signal probability.

Marwan and Kurths [41] studied about the line structures in recurrence plots. Recurrence plots exhibit line structures which represent typical behaviour of the investigated system. The local slope of these line structures is connected with a specific transformation of the time scales of different segments of the phase-space trajectory. This provides a better understanding of the structures occurring in recurrence plots. Line structures in recurrence plots and cross recurrence plots contain information about epochs of a similar evolution of segments of phase space trajectories. The local slope of such line structures is directly related with the difference in the velocity the system changes at different times. They have demonstrated that the knowledge about this relationship allows a better understanding of structures occurring in RPs. This relationship can be used to analyse changes in the time domain of data series.

Marcha, Chapmana and Dendy 2004[42] derived analytical expressions which relate the values of key statistics, notably determinism and entropy of line length distribution, to the correlation sum as a function of embedding dimension. These expressions are obtained by deriving the transformation which generates an embedded recurrence plot from an unembedded plot. A single unembedded recurrence plot thus provides the statistics of all possible embedded recurrence plots. If the correlation sum scales exponentially with embedding dimension, it can be shown that these statistics are determined entirely by the exponent of the exponential. They also examine the relationship between the mutual information content of two timeseries and the common recurrent structure seen in their recurrence plots. This allows time-localized contributions to mutual information to be visualized.

Schinkel, Dimigen, and Marwan 2008 [43] addressed one key problem in applying RPs and RQA, which is the selection of suitable parameters for the data under investigation. In this paper they addressed the issue of threshold selection in RP/RQA. The core criterion for choosing a threshold is the power in signal detection that threshold yields. They have validated their approach by applying it to model as well as to a real-life data.

Webber Jr. et al. [44] explained about the application of Recurrence Quantification Analysis as a general purpose data analysis tool. RQA has become a general purpose technique allowing for generating models endowed with a theoretical appeal in virtually any science fields, starting with cardiology and other

life sciences, over engineering, economics, astrophysics and up to Earth sciences. The importance of recurrence analysis (RQA) over spectral analysis (FFT) was successfully carried out by comparing performances of the two methodologies on the exact same, real-world time signal.

Mocenni, Facchini and Vicino [45] have done a comparative study of the recurrence properties of time series and two-dimensional spatial data is performed by means of RQA. The measures determinism and entropy provide significant information about the small and large scale characterization of the patterns allowing for a better connection to the physical properties of the spatial system under investigation.

They explored the relevance of the RQA to time series and spatially distributed systems proving that, notwithstanding several analogies, the spatial dimension introduces relevant new insights in the methodology. It has been shown that in both cases the initial part of the histogram is more informative than the tails; a saturation of DET and ENT is observed. Then critical line lengths L_{DET} and L_{ENT} can be detected, indicating a threshold length leading to the saturation of the two measures. The main disparity between the time series and spatial cases relies on the shape of the line length distribution: in the former it decays exponentially, while in the later case it may have more complex decays, depending on the occurrence of different amplitude patterns and on the finite size of the images. Moreover, the threshold line lengths L_{ENT} and L_{DET} have revealed to be different in the spatial case, especially if large patterns are present. In the time series the saturation of DET and ENT arises always for the similar critical lines. The difference between L_{ENT} and L_{DET} has been

related to different patterns size and shape. Analogously, entropy is able to account for small scale patterns, since it is more affected by shorter lines. Considering the above, it can be seen that the use of the Generalized RQA to spatially distributed systems offers new insights in the investigation of spatial patterns by using only a small number of measured data.

The cross recurrence plots (CRP), which enables the study of synchronization or time differences in two time series. This is emphasized in a distorted main diagonal in the cross recurrence plot, the line of synchronization (LOS). A non-parametrical fit of this LOS can be used to rescale the time axis of the two data series (whereby one of it is compressed or stretched) so that they are synchronized [46].

Cross recurrence plots reveal similarities in the states of the two systems. A similar trajectory evolution gives a diagonal structure in the CRP. An additional time dilatation or compression of one of these similar trajectories causes a distortion of this diagonal structure. This effect is used to look into the synchronization between both systems. Synchronized systems have diagonal structures along and in the direction of the main diagonal in the CRP. Interruptions of these structures with gaps are possible because of variations in the amplitudes of both systems. However, a loss of synchronization is viewable by the distortion of these structures along the main diagonal (LOS). By fitting a non-parametric function to the LOS one allows to re-synchronization or adjustment to both systems at the same time scale. Although this method is based on principles from deterministic dynamics, no assumptions about the underlying systems has to be made in order for the method to work.

Zbilut, Giuliani and Webber, Jr. [47] have proposed a new technique, CRQA, which demonstrates the ability to extract signals up to a very low signal-to-noise-ratio and to allow an immediate appreciation of their degree of periodicity. The lack of any stationarity dependence of the proposed method opens the way to many possible applications, including encryption. The demonstrated ability of recurrence quantification analysis to detect very subtle patterns in time series was exploited to devise a filter able to recognize and extract signals buried in large amounts of noise.

Marwan, and Kurths [48] have developed three measures of complexity mainly based on diagonal structures in CRPs. The CRP analysis of prototypical model systems with nonlinear interactions demonstrated that this technique enables them to find these nonlinear interrelations from bivariate time series, whereas linear correlation does not. Applying the CRP analysis to climatological data, they found a complex relationship between rainfall and El Niño data.

The technique of cross recurrence plots (CRPs) has modified in order to study the similarity of two different phase space trajectories. They have introduced three measures of complexity recurrence rate (RR), determinism (DET) and average diagonal line length (L) based on these distributions. These measures enable them to quantify a possible similarity and interrelation between both dynamical systems. They have demonstrated the potentials of this approach for typical model systems and natural data. In the case of linear systems, the results with this nonlinear technique agree with the linear correlation test.

Dale, Warlaumont and Richardson [49] present a lag sequential analysis for behavioural streams, a commonly used method in psychology for quantifying the relationships between two nominal time series. Cross recurrence quantification analysis (CRQA) is shown as an extension of this technique. In addition, they demonstrated nominal CRQA in a simple coupled logistic map simulation, permitting the investigation of properties of nonlinear systems such as bifurcation and onset to chaos, even in the streams obtained by coarse-graining a coupled non- linear model. They end with a summary of the importance of CRQA for exploring the relationship between two behavioural streams, and review a recent theoretical trend in the cognitive sciences. This is a guideline for applying emerging methods to coarse-grained, nominal units of measure in general properties of complex, nonlinear dynamical systems.

Vlahogianni et al. [50] investigated the effect of transitional traffic flow conditions imposed by the formation and dissipation of queues. A cross-recurrence quantification analysis combined with Bayesian augmented networks are implemented to reveal the prevailing statistical characteristics of the short-term traffic flow patterns under the effect of transitional queue conditions. Results indicate that transitions between free-flow conditions, critical queue conditions that exceed the detector's length, as well as the occurrence of spillovers impose a set of prevailing traffic flow patterns with different statistical characteristics with respect to determinism, nonlinearity, non-stationarity and laminarity. The complexity in critical queue conditions is further investigated by introducing two supplementary

regions in the critical area before spillover occurrence. Results indicate that the supplementary information on the transitional conditions in the critical area increases the accuracy of the predictive relations between the statistical characteristics of traffic flow evolution and the occurrence of transitions.

In general a lot of studies were done on RP and CRP for a wide variety of applications. However it has not reported the use of CRP for the machining purpose. Hence an attempt is made to do the analysis of machining data using CRP methods.

2.4 Chaotic Metal Cutting Process

Innovative advance of nonlinear science have thrown light to the complex and nonlinear physical systems in an extensive variety of different applications. Studies of non-linear dynamical systems for finding solutions to problems in manufacturing resulted in the applications of nonlinear dynamics to control and optimize manufacturing processes like cutting, grinding and shaping. The interdisciplinary works of physicists and mathematicians gave a better understanding of machining process.

Bukkapatnam, Lakhtakia and Kumara [51] described three independent approaches, two statistical tests and a Lyapunov exponents-based test, to establish the occurrence of low-dimensional chaos in the sensor signals from actual experiments on a lathe. It created a significant impact on views concerning the dynamics of metal cutting. They suggested that a small amount of chaos may actually be good in machining, since it introduces many scales in the surface topology.

Friction, tool wear, vibration, material flow, deformation, fracture etc. are the physical phenomena which influence the dynamics of a cutting process. Diverse material properties, cutting parameters and tool geometry can lead to appreciably dissimilar cutting dynamics. The lack of a reliable analytical description of the cutting process may be due to this. The dynamics of turning operation was assumed to be linear for earlier models developed. Later models assumed linear dynamics contaminated with additive noise. Nevertheless these models were insufficient particularly for global characterization of the turning dynamics; nonlinear models are to be resorted to.

Doi and Kato [52] offered one of the earliest nonlinear models and executed some experiments on creating chatter as a time-delay problem. Tobias [53] and Tlusty [54] and others have done substantial studies on nonlinearity. Nonlinear dynamics analysis mainly consisted of perturbation analysis and numerical simulation before 1980. Albeit time records of cutting dynamics clearly showed unsteady oscillations, random-like motions were not considered [53]. New perceptions of modeling, measuring and controlling nonlinear dynamics in material processing have appeared after 1980s. A friction model was used by Grabec [55, 56] in his ground-breaking paper on chaos in machining. The assumption that the dynamics of the turning operation may be chaotic has impelled by the observation of the complex response from the nonlinear model of Grabec [55].

Marui et al. [57] carried out pilot studies on nonlinear modelling. The existence of primary and secondary chatter were conducted by Warminski et al.

[58,59], Litak et al. [60], Pratt and Nayfeh [61], Stepan and Kalmar-Nagy [62]. The consequent experimental results, predominantly on an orthogonal cutting process, have been considered in several papers [63-65].

The nonlinear phenomena in machine tool operations involved three different approaches viz. measurement of nonlinear force-displacement behaviour of cutting or forming tools, model-based studies of bifurcations using parameter variation and time-series analysis of dynamic data for system identification.

Tobias [53] was victorious in predicting the onset of chatter with the classical model with nonlinear cutting force [66], it cannot probably explain all phenomena displayed in real cutting experiments. Single degree-of-freedom deterministic time-delay models have been insufficient so far to explain low-amplitude dynamics below the stability boundary. Also, real tools have multiple degrees of freedom. Kalmar-Nagy and Moon [67] examined the coupling between multiple degree-of-freedom tool dynamics and the regenerative effect in order to see if the chatter instability criteria will permit low-level instabilities. It was shown that this mode-coupled non conservative cutting tool model including the regenerative effect (time delay) can produce an instability criteria that admits low-level or zero chip thickness chatter.

Oxley and Hastings [68] studied about steady-state forces as functions of chip thickness, as well as cutting velocity for carbon steel. They considered a reduction of cutting force versus material flow velocity in steel. the cutting forces for different tool rake angles were also measured. These relations were used by Grabec [55, 56]

to put forward a non-regenerative two-degree of freedom model for cutting that envisage chaotic dynamics. Nonetheless, the force measurements themselves are quasi-steady and were taken to be single-valued functions of chip thickness and material flow velocity.

The critical values of the control parameter at which the dynamics topology changes permit the researcher to relate the model behaviour with experimental observation in the actual process. These studies permit one to design controllers to suppress unnecessary dynamics or to change a sub critical Hopf bifurcation into a supercritical one. The phase-space methodology also provides itself to new diagnostic tools, such as Poincar´e maps, which can be employed to glance for changes in the process dynamics [69,70]. The limitations of the model-based bifurcation approach are that the models are usually crude and not founded on fundamental physics. The use of bifurcation tools was most effective when the phase-space dimension is small, say, less than or equal to four.

Abarbanel [71] used the time-series analysis method to analyze many dynamic physical phenomena like ocean waves, heartbeats, lasers and machine-tool cutting. This method was based on the use of a series of digitally sampled data, from which an orbit in a pseudo-M-dimensional phase space was constructed. The principal objectives of this method is to place a bound on the dimension of the underlying phase space from which the dynamic data were sampled. This can be done with several statistical methods, including fractal dimension, false nearest neighbours (FNN), Lyapunov exponents, wavelets and several others. Still, if model-based

analysis can be criticized for its simplistic models, the nonlinear time-series analysis can be criticized for its assumed generality. It is dependent on the data alone. Thus the results may be sensitive to the time delay of the sampling, the number of data points in the sampling , the signal-to-noise ratio of the source measurement, signal - filtering, , and whether the sensor captures the essential dynamics of the process. The primary objective of the machining is to have a good surface finish without sacrificing the productivity. Cutting below the chatter threshold is required for this. Below this threshold, linear models predict no self-excited motion. Yet when cutting tools are instrumented, one can see random-like bursts of oscillations with a centre frequency near the tool natural frequency. Johnson [69] has shown that these vibrations are significantly above any machine noise in a lathe-turning operation. These observations have been done by several laboratories, and time-series methodology has been used to diagnose the data to determine whether the signals are random or deterministic chaos [51, 69, 72-82]. These experiments and others (Bukkapatnam et al.) suggest that normal cutting operations may be naturally chaotic.

In order to study these chaotic effects arising out of the non linear nature of the cutting process, no attempt has been reported based on the cross recurrence plot based analysis.

2.5 Summary

The nonlinear analysis concedes the essential dynamic character of material removable processes. It is necessary to integrate the different methods of research, such as bifurcation theory, cutting-force characterization and time-series analysis, before nonlinear dynamics modelling can be made functional. In this thesis work a modest attempt is made to apply CRQA methods to coupling systems and to provide a new methodology for detection of chatter in metal cutting. The methodology stems from nonlinear time series analysis and is based on Cross Recurrence Plots.

This chapter gives a general overview of the current scenario in the field of coupling research, chatter and application of cross recurrence analysis. The next chapter gives a frame work for the experiments to be conducted further.

3. Experimental Framework and Research Methodology

The theory behind the cross recurrence analysis and the research methodology adopted in this work is explained here. In many signal processing tools, the signals are supposed to be Gaussian, stationary, linear with high signal to noise ratio. However in real world systems, it is not so. The CRQA methodology is suitable for analyzing signals that do not fall into the above categories.

3.1 Time Series Analysis

A time series is a sequence of data points, measured typically at successive times spaced at uniform time intervals. Time series analysis comprises of methods for analyzing time series data in order to extract meaningful statistics and other characteristics of the data.

In nature many quantities fluctuate in time and it is assumed to be a consequence of random and unpredictable events. It is now understood that some of these cases may be a result of deterministic chaos and hence predictable in the short term and responsive to simple modelling.

Nonlinear time series analysis (NTSA) began to attract serious attention due to the realisation that linear time series models are incapable of reflecting many important real phenomena. Poincare [85] stated unequivocally that one fundamental source of randomness is the initial-value sensitivity of a dynamical system. Hence even a deterministic dynamical system can generate randomness as long as it is sensitive to initial values.

A brief comparison of linear and nonlinear methods [71] is given in Table 3.1. If the current state of the system is known, the future state x_{n+t} can be determined precisely from the current state x_n at any instance n for some value of $t>0$ by applying the deterministic rule for the dynamical system. It is important to identify the stationarity of the dynamical system. If the dynamical system is not stationary, it is difficult to model it from time series. Unless one has a prior knowledge of the structure of the underlying system, the number of parameters will greatly exceed the number of available data [86].

The dynamics of the system are to be obtainable in a phase space to apply the nonlinear time series methods to a dynamical system which is both stationary and deterministic. The first step in this procedure is the attractor reconstruction, the time delayed embedding of the data. The appropriate embedding delay and embedding dimension are to be determined.

Table 3.1. Comparison of signal processing techniques [71]

Linear signal processing	Nonlinear signal processing
Finding the signal:	***Finding the signal:***
Separate broadband noise from narrowband signal using spectral characteristics. Method: Matched filter in frequency domain.	Separate broadband signal from broadband noise using the deterministic nature of the signal. Method: Manifold decomposition or statistics on the attractor.
Finding the space:	***Finding the space:***
Use Fourier space methods to turn differential equations into algebraic forms	Time lagged variables form coordinates for a reconstructed state space in m dimensions.
$x(t)$ is observed $X(f) = \sum x(t) e^{i2\pi f}$ is used	$X(t) = [x(t),\ \mathrm{x}(t+\tau),\ \mathrm{x}(t+2\tau), \ldots\ldots x(t+(m-1)\tau)]$ where τ and m are determined by false nearest neighbours and average mutual information.
Classify the signal:	***Classify the signal:***
• Sharp spectral peaks • Resonant frequencies of the system	• Lyapunov exponents • Fractal dimension measures • Unstable fixed points • **Recurrence quantification** • Statistical distribution of the attractor
Making models, predict:	***Making models, predict:***
$x(t+1) = \sum \alpha_k x(t-k)$ Find parameters α_k consistent with invariant classifiers – location of spectral peaks.	$X(t) \to X(t+1)$ $X(t+1) = F\left[X(t), a_1, a_2, \ldots\ldots a_p\right]$ Find parameters a_j consistent with invariant classifier – Lyapunov exponents, fractal dimensions.

The average mutual information method [87] yields an estimate for the proper embedding delay and the false nearest neighbour method [88] enables us to determine a proper embedding dimension.

3.2 Analysis of Phase Space Trajectories

The analysis of phase space trajectories is a basic concept of non linear data analysis. A dynamical system is given by a phase space, a continuous or discrete time and a time evolution law. The elements of the phase space represent possible states of the system [91]. A signal contains information about unobserved state variables which can be used to predict the present state. Hence a scalar time series $\{x\,(i)\}$ may be used to construct a vector time series that is equivalent to the original dynamics from a topological point of view.

Packard et al. [89] conducted experiments associating the phase space or state space vector of dynamical variables of the physical system to the time series measured. They proved that it was possible to reconstruct a multidimensional state-space vector $X\,(i)$ by using time delays with the measured, scalar time series, $\{x\,(j)\}$. Takens [90] and later Sauer et al. [91] put this idea on a mathematically sound footing by proving a theorem which forms the basis for the methodology of delays. It is shown that the equivalent phase space trajectory preserves the topological structures of the original phase space trajectory. Because of this dynamical and topological equivalence, the characterization and prediction based on the reconstructed state space is as valid as in the true state space. The reconstructed attractor can be characterized by a set of static and dynamic characteristics. The dynamical characteristics describe the dynamical properties of nearby trajectories in phase space and the static characteristics describe the geometrical properties of the attractor.

Given a time series $\{x(j) = x(1), x(2), x(3), \ldots \ldots . . x(N)$

Points $X(i)$ in an *m* -dimensional state space is defined as

$X(i) = [x(i), x(i+\tau), x(i+2\tau), \ldots\ldots\ldots\ x(i+(m-1)\tau)]$

For $i = 1,2,3, \ldots \ldots, \mathrm{N} - (m-1)\tau$

where i are time indices, τ, a time delay or embedding delay, and m the embedding dimension. Time evolution of $X\ (i)$ is called a trajectory of the system, and the space which this trajectory evolves is called the embedding space.

The proper selection of appropriate embedding parameters τ and m is imperative. In practice the origin of the time series may be an unknown system. Then it is impossible to know the degrees of freedom of the underlying dynamics that produced the time series. The time required for checking all possibilities that might yield a proper embedding with respect to various τ and m is very long. Hence there is a need to depend on average mutual information method and the false nearest neighbour method, which facilitate us to efficiently determine proper values of the embedding delay τ and embedding dimension m.

3.3 False Nearest Neighbours (FNN) Method

The objective of selecting an embedding dimension is to make adequate observations so that the deterministic state of the system can be resolved unambiguously. In the presence of observational noise and finite quantization this is not possible. A correct embedding dimension will yield a set of states indistinguishable from the true state [92]. The aim of estimating the embedding

dimension is to achieve unambiguity of the system state. The prime example of many of these methods is the False Nearest Neighbours (FNN) technique [93-94].

Kennel et al. [88] introduced the false nearest neighbour method as an efficient tool for determining the minimal required embedding dimension m in order to fully resolve the complex structure of the attractor, i.e. the minimum dimension at which the reconstructed attractor can be considered completely unfolded. An acceptable minimum embedding dimension can be determined by looking at the behaviour of near neighbours under changes in the embedding dimension from d to d+1. When the number of nearest neighbours arising through projection is zero in dimension d_E, the attractor has been unfolded in this dimension.

Takens [90] introduced the embedding theorem which guarantees a proper embedding for all large enough m, that is larger than the minimal required embedding dimension. The method can be seen as an optimization procedure yielding just the minimal required m. It depends on the supposition that an attractor of a deterministic system folds and unfolds smoothly with no sudden irregularities in its structure. By utilizing this hypothesis, it can be concluded that the two points that are close in the reconstructed embedding space have to stay sufficiently close also during forward iteration. If this criterion is fulfilled, then after some sufficiently short forward iteration, the distance between two points $X(n)$ and $X(p)$ of the reconstructed attractor, cannot grow further as a threshold value is fixed for these distances in computation. But if an n^{th} point has a close neighbour that doesn't fulfil this criterion, then this n^{th} point is marked as having a false nearest neighbour. The

fraction of points having a false nearest neighbour is to be minimized by choosing a sufficiently large m.

As explicated above, if m is chosen very small, it is difficult to collect enough information about other variables that influence the value of the measured variable to successfully reconstruct the whole phase space. From the geometrical point of view, this means that two points of the attractor might solely appear to be close, whereas under forward iteration, they are mapped randomly due to projection effects. The random mapping occurs because the whole attractor is projected onto a hyper plane that has a smaller dimensionality than the actual phase space and so the distances between points become distorted [95].

For computing the fraction of false nearest neighbours, the following algorithm is used.

- Consider each vector $X(n) = [x(n),\ \mathrm{x}(n+\tau),\ \mathrm{x}(n+2\tau),.....x(n+(m-1)\tau)]$ in a delay coordinate embedding of the time series with delay τ and embedding dimension m. Seek its nearest neighbour $X(p) = [x(p),\ \mathrm{x}(p+\tau),\ \mathrm{x}(p+2\tau),.....x(p+(m-1)\tau)]$. The nearest neighbour is determined by finding the vector $X(p)$ in the embedding which minimizes the Euclidean distance $R_n = \|X(n) - X(p)\|$.
- Now consider each of these vectors in an m+1 dimensional embedding,

$$X'(n) = [x(n),\ \mathrm{x}(n+\tau),\ \mathrm{x}(n+2\tau),.....x(n+(m-1)\tau), x(n+m\tau)]$$

$$X'(p) = [x(p),\ \mathrm{x}(p+\tau),\ \mathrm{x}(p+2\tau),.....,x(p+(m-1)\tau), x(p+m\tau)]$$

- In an $m+1$ dimensional embedding, these vectors are separated by the Euclidean distance $R'_n = \left\| X'(n) - X'(p) \right\|$. The first criterion by which Kennel et al.[88], identify a false nearest neighbour is

Criterion 1: $$\left[\frac{R'^2_n - R^2_n}{R^2_n} \right]^{1/2} = \frac{\left| x(n+m\tau) - x(p+m\tau) \right|}{R_n} > R_{tol} \quad (1)$$

R_{tol} is a unitless tolerance level for which Kennel et al.[88], suggest a value of approximately 15. This criterion is meant to measure if the relative increase in the distance between two points when going from m to $m+1$ dimensions is large. The value 15 was suggested based upon empirical studies of several systems, although values between 10 and 40 were generally acceptable [96].

- The other criterion Kennel et al.[88], suggest is

Criterion 2: $$\left[\frac{R'_n}{R_A} \right] > A_{tol} \quad (2)$$

This compensates for the fact that portions of the attractor may be quite sparse. In those regions, near neighbours are not actually close to each other. Here, R_A is a measure of the size of the attractor, for which Kennel et al.[88], use the standard deviation of the data. If either of the criterions hold, then $X(p)$ is considered a false nearest neighbour of $X(n)$. The total number of false nearest neighbours is found, and the percentage of false nearest neighbours, out of all nearest neighbours, is measured. An appropriate embedding dimension is one where the percentage of false nearest neighbours identified by either method falls to zero.

This criterion perfectly recognizes an appropriate embedding dimension in most cases. With the above information, embedding space can be successfully

reconstructed from an observed variable. In order to yield meaningful results, all methods of nonlinear time series analysis must accomplish this step successfully.

Once the embedding dimension has been assessed properly, time delay has to be considered. Identifying a proper delay τ for the observed time series is an important undertaking.

3.4 Average Mutual Information (AMI) Method

The mutual information of two random variables is a quantity that measures the mutual dependence of the two random variables. A suitable embedding delay τ has to fulfil two criteria. First, τ has to be large enough so that the information gathered from measuring the value of x variable at time $(\mathrm{i}+\tau)$ is relevant and significantly different from the available information, by knowing the value of the measured variable at time i. Only then it will be possible to gather enough information about all other variables that influence the value of the measured variable to successfully reconstruct the whole phase space with a reasonable choice of m. Note here that generally a shorter embedding delay can always be compensated with a larger embedding dimension.

This is the rationale why the original embedding theorem is formulated with respect to m, and says basically nothing about τ. It has to be ensured that τ should not be larger than the typical time in which the system looses memory of its initial state. If a large value for τ is chosen, the reconstructed phase space would look more or less random since it would consist of uncorrelated points. The later condition is

important for chaotic systems which are intrinsically unpredictable and, therefore loose memory of the initial state as time progresses. This second demand has led to suggestions that a proper embedding delay could be estimated from the autocorrelation function where the optimal τ would be determined by the time the autocorrelation function first decreases below zero or decays to $1/e$. For nearly regular time series, this is a good thumb rule, whereas for chaotic time series, it might lead to spurious results since it based solely on linear statistic and doesn't take into account nonlinear correlations.

Fraser and Swinney [97] introduced a method for solving this issue. They ascertained that delay corresponds to the first local minimum of the average mutual information function $I(\tau)$ which is defined as follows:

$$I(\tau) = \sum P(x(i), x(i+\tau)) \log_2 \left[\frac{P(x(i), x(i+\tau))}{P(x(i))P(x(i+\tau))} \right] \quad (3)$$

where $P(x(i))$, is the probability of the measure $x(i)$, $P(x(i+\tau))$ is the probability of the measure $x(i+\tau)$ and $P(x(i), x(i+\tau))$ is the joint probability of the measure of $x(i)$ and $x(i+\tau)$ [96]. The average mutual information is really a kind of generalization to the nonlinear phenomena from the correlation function in the linear phenomena. When the measures $x(i)$ and $x(i+\tau)$ are completely independent, $I(\tau) = 0$. On the other hand when $x(i)$ and $x(i+\tau)$ are equal, $I(\tau)$ is maximum. Therefore plotting $I(\tau)$ versus τ is likely to identify the preeminent value for the time delay, which is associated to the first local minimum.

The first minimum of $I(\tau)$ yields the optimal embedding delay, the proof of this has a more insightful background. It is stated that at the embedding delay where $I(\tau)$ has the first local minimum, $x(i+\tau)$ appends the largest amount of information to the information gathered by identifying $x(i)$, without completely losing the correlation between them.

Shaw [98] presents a more persuasive substantiation of this being true. However a formal mathematical proof is lacking. Kantz and Schreiber [99] also report that in fact there is no theoretical reason why there should even exist a minimum of the mutual information. However, this should not weaken the dependability in this particular method, since it has often proved reliable and well suited for the chosen task.

3.5 CRP based Time Series Analysis

State space reconstruction (SSR) from single time series has been a powerful approach for the analysis of the complex, non-linear systems that appear ubiquitous in the natural and human world. The main shortcoming of this method is the phenomenological nature of attractor reconstructions. Additionally, applied studies show that these single time series reconstructions can often be improved *ad hoc* by including multiple dynamically coupled time series in the reconstructions, to provide a more mechanistic model.

For natural systems recurrent behaviours is typical. In the construction of dynamical systems, this implies the recurrence of state vectors, i.e. states with large temporal

distances may be close in state space. This is typical for nonlinear or chaotic systems and a well-known property of deterministic dynamical systems.

Henri Poincare [85] introduced the concept of recurrences in his influential work in 1890. Even though much mathematical work was carried out in the following years, Poincare's pioneering work and his discovery of recurrence had to wait for more than 70 years for the development of fast and efficient computers to be exploited numerically. The use of powerful computers boosted chaos theory and allowed to study new and exciting systems. Some of the tedious computations needed to use the concept of recurrence for more practical purposes could only be made with this digital tool. In 1987, Eckmann et al.[100] for the first time, introduced the method of RPs to visualize the recurrences of dynamical systems in a phase space.

3.6 Creation of Recurrence Plot

The phase spaces of more than two dimensions can only be envisaged by a projection, it is tough to explore recurrences in the state space. In the RP, any recurrence of state i with state j is depicted on a Boolean matrix is expressed by

$$RP(i,j) = \Theta(\varepsilon - \|X(i) - X(j)\|), \quad i,j = 1,2,\ldots\ldots,N \tag{4}$$

$X(i)$ and $X(j)$ are the embedded vectors, i and j are time indices, N is the number of measured points, $\|\cdot\|$ is a norm, and ε is an arbitrary threshold radius and $\Theta(.)$ is the Heaviside step function($\Theta(X) = 0$, if $X < 0$ and $\Theta(X) = 1$ if $X \geq 0$).

The RP is attained by plotting the recurrence matrix, Eq. (4), and using different colours for its binary entries, e.g., plotting a black dot at the coordinates (i,j), if

$RP(i,j)=1$, and a white dot, $RP(i,j)=0$. Both axes of the RP are time axes and show rightwards and upwards (convention). Since any state is recurrent with itself , the RP matrix fulfils $RP(i,i)=1|_{i=1}^{N}$ by definition, the RP has always a black main diagonal line called the line of identity (LOI). Additionally, the RP is symmetric by definition with respect to the main diagonal, i.e. $RP(i,j)=RP(j,i)$.

An appropriate norm has to be selected to compute an RP. The norm function geometrically defines the size (and shape) of the neighbourhood surrounding each reference point. The commonly used norms are the L_1-norm, the L_2-norm (Euclidean norm) and the L_∞-norm (Maximum or Supremum norm). The neighbourhoods of these norms have different shapes (Figure 3.1). Considering a fixed ε, the L_∞-norm finds the most, the L_1-norm the least and the L_2-norm an intermediate amount of neighbours[101]. Since a vector must have at least two points, each norm is unique if and only if $m>1$, else all norms are exactly equivalent for $m=1$. Computed distance values are distributed within a distance matrix, DM of size WxW, where $W=N-m+1$The distance matrix DM has W^2 elements with a long central diagonal of W distances all equal to 0. This value of W is valid for a delay of 1. A universal value for W is then $W=N-(m-1)\tau$. The Recurrence matrix RM is derived from $DM$by setting the threshold radius, ε. The Heaviside function assigns values of 0 or 1 to array elements in the RM. Only those distances in $RM(i,j)$ equal to or less than ε are defined as recurrent points at coordinates (i,j).

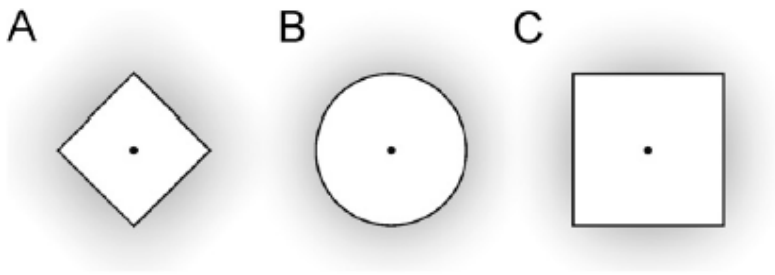

Fig. 3.1 Three commonly used norms for the neighbourhood with the same radius around a point (black dot) exemplarily shown for the two-dimensional phase space: (A) L_1 -norm, (B) L_2 -norm and (C) L_∞ -norm.

3.7 *Neighbourhood Threshold*

A critical factor of an RP is the threshold radius ε. Special consideration has to be given for its selection. If ε is chosen too small, there may be almost no recurrence points and no information about the recurrence structure of the underlying system is obtained. On the other hand, if ε is chosen too large, almost every point is a neighbour of every other point, which leads to a lot of artifacts. A too huge ε includes points into the neighbourhood which are consecutive points on the trajectory. This effect is called tangential motion and causes thicker and longer diagonal structures in the RP as they actually are. Hence, compromise has to found for the value of ε. The "shotgun plot" of Figure 3.2 [33] provides a conceptual framework for understanding why an increasing threshold radius captures more and more recurrent points in phase space. For simplicity, in this thesis the threshold radius will be referred to as RADIUS.

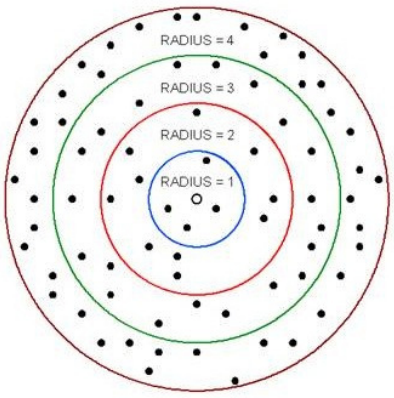

Fig. 3.2 Shot gun plot representation of a hypothetical system in higher-dimensional phase space with a splay of points (closed dots) surrounding a single reference point (open dot). The points falling within the smallest circle (RADIUS = 1 distance units) are the nearest neighbours of the reference point. That is, those points are recurrent with the reference point. The second concentric circle (RADIUS = 2 distance units) includes a few more neighbours, increasing the number of recurrences from 4 to 14. Increasing the radius further (RADIUS = 3 or 4 distance units) becomes too inclusive, capturing an additional 20 or 60 distant points as nearest neighbours when, in fact, they are not [33].

3.8 Quantification of Recurrence Plots

The purpose of recurrence plots was to envisage trajectories in phase space, which is especially beneficial in the case of high dimensional systems. RPs and CRPs yield important insights into the time evolution of these trajectories, because typical patterns in RPs are correlated to a specific behaviour of the system. Large scale patterns in RPs, designated in [100] as typology, can be classified in homogeneous, periodic, drift and disrupted ones [100,101]:

- Homogeneous RPs are typical of stationary systems in which the relaxation times are short in comparison with the time spanned by the RP. An example of such an RP is that of a stationary random time series.
- Periodic and quasi-periodic systems have RPs with diagonal oriented, periodic or quasi-periodic recurrent structures (diagonal lines, checkerboard structures). Irrational frequency ratios cause more complex quasi-periodic recurrent structures (the distances between the diagonal lines are different).

However, even for oscillating systems whose oscillations are not easily recognizable, RPs can be useful

- A drift is caused by systems with slowly varying parameters, i.e. non-stationary systems. The RP pales away from the LOI.
- Abrupt changes in the dynamics as well as extreme events cause white areas or bands in the RP. RPs allow finding and assessing extreme and rare events easily by using the frequency of their recurrences.

A critical examination of the RPs and CRPs reveals small-scale structures, the texture which can be typically classified in single dots, diagonal lines as well as vertical and horizontal lines (the combination of vertical and horizontal lines forms rectangular clusters of recurrence points). Moreover, even bowed lines may occur [100,101]. Table 3.2 details typical patterns in RPs and their meanings

- Single, isolated recurrence points can occur if states are rare, if they persist only for a very short time, or fluctuate strongly.
- A diagonal line $R(i+k, j+k) \equiv 1_{k=0}^{l-1}$ (where l is the length of the diagonal line) occurs when a segment of the trajectory runs almost in parallel to another segment (i.e. through an ε-tube around the other segment, Figure 3.3) for l time units. The length of this diagonal line is determined by the duration of such similar local evolution of the trajectory segments. The direction of these diagonal structures is parallel to the LOI (slope one, angle $\pi/4$). They

represent trajectories which evolve through the same ε-tube for a certain time.

- A vertical (horizontal) line $R(i, j+k) \equiv 1_{k=0}^{v-1}$ (with $v$the length of the vertical line) marks a time interval in which a state does not change or changes very slowly. Hence, the state is trapped for some time. This is a typical behaviour of laminar states (intermittency) [102].

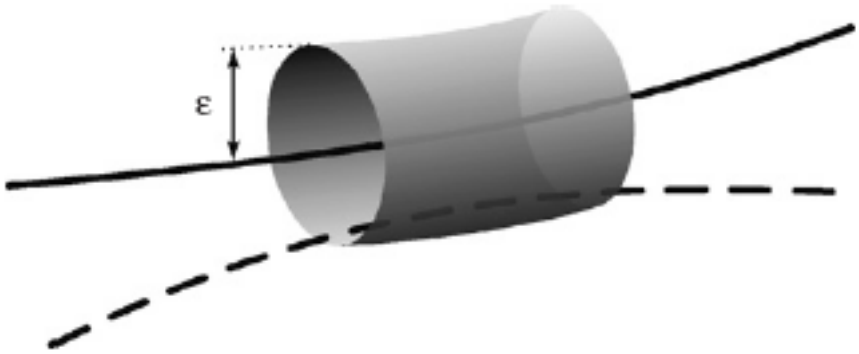

Fig. 3.3 A diagonal line in a RP corresponds with a section of a trajectory (dashed) which stays within an ε-tube around another section (solid).

- Bowed lines are lines with a non-constant slope. The shape of a bowed line depends on the local time relationship between the corresponding close trajectory segments.

Table 3.2 Typical patterns in RPs and their meanings

	Pattern	Meaning
1	Homogeneity	The process is stationary
2	Fading to the upper left and lower right corners	Non-stationary data; the process contains a trend or a drift
3	Disruptions (white bands)	Non-stationary data; some states are rare or far from the normal; transitions may have occurred.
4	Periodic/quasi-periodic patterns	Cyclicities in the process; the time distance between periodic patterns (e.g. lines) corresponds to the period; different distances between long diagonal lines reveal quasi-periodic processes
5	Single isolated points	Strong fluctuation in the process; if only single isolated points occur, the process may be an uncorrelated random or even anti-correlated process
6	Diagonal lines (parallel to the LOI)	The evolution of states is similar at different epochs; the process could be deterministic; if these diagonal lines occur beside single isolated points, the process could be chaotic (if these diagonal lines are periodic, unstable periodic orbits can be observed)
7	Diagonal lines (orthogonal to the LOI)	The evolution of states is similar at different times but with reverse time; sometimes this is an indication for an insufficient embedding
8	vertical and horizontal lines/clusters	Some states do not change or change slowly for some time; indication for laminar states
9	Long bowed line structures	The evolution of states is similar at different epochs but with different velocity; the dynamics of the system could be changing

Without some skill, it is not easy to visually analyse the RPs. RPs of paradigmatic systems provide an informative introduction into characteristic typology and texture. The majority of these patterns are also seen in cross recurrence plots. However, a quantification of the obtained structures is necessary for a more objective investigation of the considered system.

3.9 Cross Recurrence Quantification Analysis

Analysis of RPs and CRPs is subjective as individual biases of multiple observers and subjective interpretations of the plots results in the outcome. Specific rules had to be

devised whereby certain recurrence features could be automatically extracted from CRPs to avoid the above problems.

Numerous measures of complexity which quantify the small-scale structures in RPs and CRPs have been proposed [102-104] with a purpose to go beyond the visual feeling yielded by individuals. These are known as CRQA variables. These measures are based on the recurrence point density and the diagonal and vertical line structures of the CRP. A computation of these measures in small windows or otherwise called epochs (sub-matrices) of the CRP yields the time dependent behaviour of these variables. Various studies based on CRQA measures show that they are able to measuring interpersonal coordination in the context of Conversation [105]. The vertical structures in the CRP are related to intermittency and laminar states. Those measures quantifying the vertical structures enable also to detect chaos–chaos transitions [102].

Unlike RP, the CRP is not symmetrical across the central diagonal. Hence a quantitative feature extraction has to be done considering the whole CRP. Following statistical values can be derived from a CRP using CRQA. The first value is percent recurrence(%REC), quantifies the percentage of recurrent points falling within the specified radius. For a given window size W ,

$$Percent\ recurrence = \frac{No.of\ recurrent\ points * 100}{(W(W-1)/2)} \quad (5)$$

Here W refers to the recurrence window size after accounting for embedding and delay; ie. $W = [(N_2 - N_1 + 1) - (m-1)\tau]$ where N_1 and N_2 are the first and last points of the window considered.

The second variable is percent determinism (%DET) and measures the percentage of recurrent points that are contained in lines parallel to the main diagonal of the RP, which are known as deterministic lines. A deterministic line is defined if it contains a predefined minimum number of recurrence points. It represents a measure of predictability of the system.

$$Percent\ determinism = \frac{Number\ of\ points\ in\ diagonal\ lines\ *\ 100}{Number\ of\ recurrence\ points} \quad (6)$$

The third recurrence variable is Linemax (LMAX), which is simply the length of the longest diagonal line segment in the plot, excluding the main diagonal LOI (where $i = j$). This is a very important recurrence variable because it inversely scales with the most positive Lyapunov exponent [100,105]. Positive Lyapunov exponents gauge the rate at which trajectories diverge, and are the hallmark for dynamic chaos.

$$Linemax = length\ of\ longest\ diagonal\ line\ in\ recurrence\ plot \quad (7)$$

The fourth variable value is called entropy(ENT) and it refers to the Shannon entropy of the distribution probability of the diagonal lines length. ENT is a measure of signal complexity and is calibrated in units of bits/bin and is calculated by binning the deterministic lines according to their length. Individual histogram bin probabilities (P_{bin}) are computed for each non-zero bin and then summed according to Shannon's equation.

$$Entropy = -\sum(P_{bin})\log_2(P_{bin}) \quad (8)$$

The fifth statistical value is the Trend (TND) which is used to detect non-stationarity in the data. The trend essentially measures how quickly the RP pales away from the main diagonal and can be utilized as a measure of stationarity. If recurrent points are homogeneously distributed across the RP, TND values will hover near zero units. If recurrent points are heterogeneously distributed across the RP, TND values will deviate from zero units. TND is computed as the slope of the least squares regression of percent local recurrence as a function of the orthogonal displacement from the central diagonal. Multiplying by 1000 increases the gain of the TND variable.

$$Trend = 1000(slope\ of\ percent\ local\ recurrence\ vs.\ displacement) \quad (9)$$

For the detection of chaos-chaos transitions, Marwan et al. [102] introduced other two additional CRQA variables, the Percent Laminarity(%LAM) and Trapping time(TT), in which attention is focused on vertical line structures and black patches. %LAM is analogous to %DET except that it measures the percentage of recurrent points comprising vertical line structures rather than diagonal line structures. The line parameter still governs the minimum length of vertical lines to be included.

$$Percent\ Laminarity = \frac{Number\ of\ points\ in\ vertical\ lines*100}{Number\ of\ recurrent\ points} \quad (10)$$

TT on the other hand is the average length of vertical line structures. It represents the average time in which the system is "trapped" in a specific state.

$$Trapping\ time = average\ length\ of\ vertical\ lines \geq parameter\ line \quad (11)$$

The eighth recurrence variable is VMAX, which is simply the length of the longest diagonal line segment in the plot. This variable is analogous to the standard measure LMAX

$$Vmax = length\ of\ longest\ vertical\ line\ in\ recurrence\ plot \quad (12)$$

3.10 Estimation of Threshold Radius

Selecting the proper threshold radius is a major step in the analysis of cross recurrence quantification. The following methods are followed for the estimation of threshold radius.

(i) RADIUS must fall with the linear scaling region of the double logarithmic plot;

(ii) %REC must be kept low (e.g., 0.1 to 2.0%); and

(iii) RADIUS may or may not coincide with the first minimum hitch in %DET.

Considering all three factors collectively, a radius of 15% was selected for the example data (vertical dashed lines in Figure 3.4) [33], which fits all three criteria. There are mathematical scaling regulations connecting log (%REC) with log (RADIUS), the first guideline for RADIUS selection is preferred. Since there are no known rules describing the hitch region in %DET, this latter method must be applied with caution. However, the choice of ε depends robustly on the considered system.

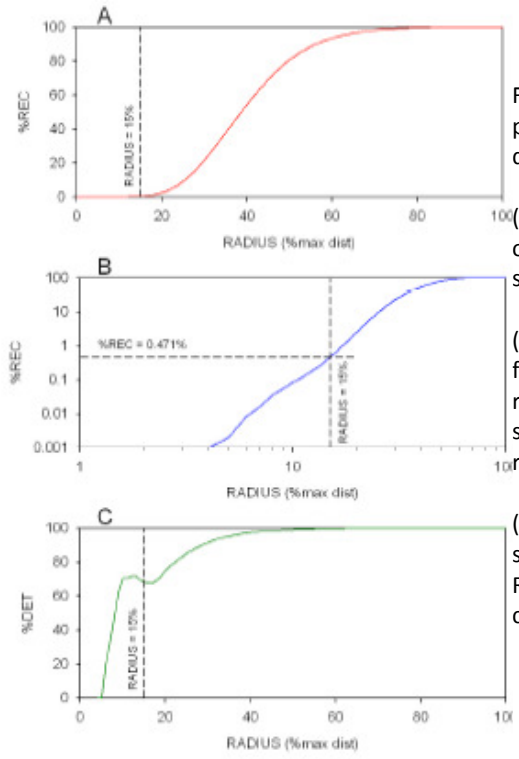

Fig. 3.4 Methods for selecting the proper radius parameter for recurrence analysis of a sample data[33]

(A) With step increases in RADIUS, the density of recurrence points (%REC) increases along a sigmoid curve (M = 10).

(B) Double-logarithmic plot of %REC as a function of RADIUS defines a linear scaling region from RADIUS = 8% to 15%. RADIUS is selected at 15% where %REC is 0.471% (sparse recurrence matrix).

(C) Linear plot of %DET as a function of RADIUS showing a short plateau and small trough near RADIUS = 15% which may or may not be coincidental.

3.11 Episodic Recurrence analysis

It is demonstrated that time series data can be embedded into higher dimensional space by the method of time delays (Takens, 1981). A distance matrix is constructed by computing distances between all possible vectors, specific distance values being based on the selected norm parameter. A recurrence matrix (RM) is created from the distance matrix (DM) by selecting a threshold radius parameter such that only a small percentage of points with small distances are counted as recurrent (yielding a sparse RM). The RP, of course, is just the graphical representations of RM elements at or below the threshold radius. Eight features (recurrence variables) are extracted from the RP within each window (W) of observation on the time series. The

question before us now is how can these recurrence variables be useful in the diagnosis of dynamical systems?

Any dynamic is sampled, Weare taking a “slice of life,” as it were. The dynamic was “alive” before Wesampled it, and probably remained “alive” after our sampling. Consider, for example, the EMG signal recorded from the biceps muscle of a normal human volunteer and its attendant RP in Figure 3.5 [106]. The focus is on the first 1972 points of the time series digitized at 1000 Hz (displayed from 37 ms to 1828 ms). But how might these digitized data be processed in terms of recurrence analysis? It would certainly be feasible to perform CRQA within the entire window (W_{last} = 1972 points) as represented by the single, large, outer RM square. On the other hand, the data can be windowed into four smaller segments (W_{small} = 1024 points) as represented by the four smaller and overlapping RM squares. In the latter case the window offset of 256 points means the sliding window jogs over 256 points (256 ms) between windows. Two effects are at play here. First, larger windows focus on global dynamics (longer time frame) whereas smaller windows focus on local dynamics (shorter time frame). Second, larger window offsets yield lower time resolution CRQA variables, whereas smaller window offsets yield higher time-resolution variables. Eight CRQA variables are computed (extracted) from each RM (or RP).

By implementing a sliding window design(termed epochs), each of those variables is computed multiple times, creating seven new derivative dynamical systems expressed in terms of %REC, %DET, LMAX, ENT, %LAM and TT. Alignment of those

variables (outputs) with the original time series (input) (adjusting for the embedding dimension, m) might reveal details not obvious in the 1- dimensional input data. This EMG example illustrates the power of sliding recurrence windows.

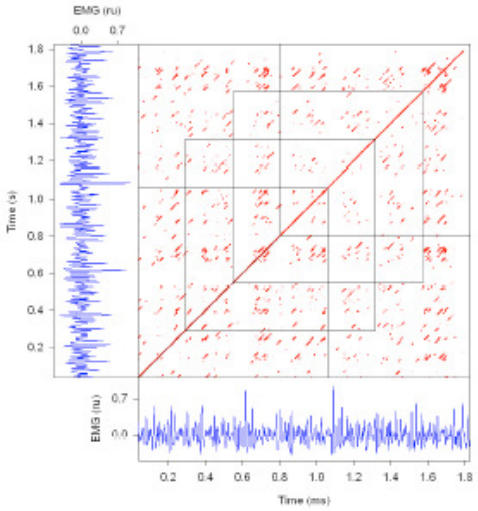

Fig. 3.5 Windowed cross recurrence analysis of EMG signal. The large outer square displays the large scale recurrence plot (W = 1792 = N points). The four small inner squares (epochs) block off the small scale recurrence plots (W = 1024 < N) with an offset of 256 points between windows. [33]

3.12 Research Methodology

For data analysis and feature extraction CRQA based methodology can be used (Figure 3.6). Attractor reconstruction is done on the recorded time series data (sensor signals) representing value fluctuations in two state variables. These are converted into a sequence of points in a higher-dimensional space by applying the Taken's time-lag embedding theorem. A symmetric matrix called distance matrix is then obtained from the points on the trajectory of this attractor. An appropriate threshold radius is fixed and using a heaviside function, the above distance matrix is transformed into a recurrence matrix. The CRP is obtained by plotting the recurrence matrices which shows all the recurrent points as dark spots. The distances in the recurrence matrix that are equal to or less than the threshold radius are taken as

recurrent points. The quantification of cross recurrence plots is based on the line structure of the plot. The CRQA gives values of a number of measures of complexity called CRQA variables, which

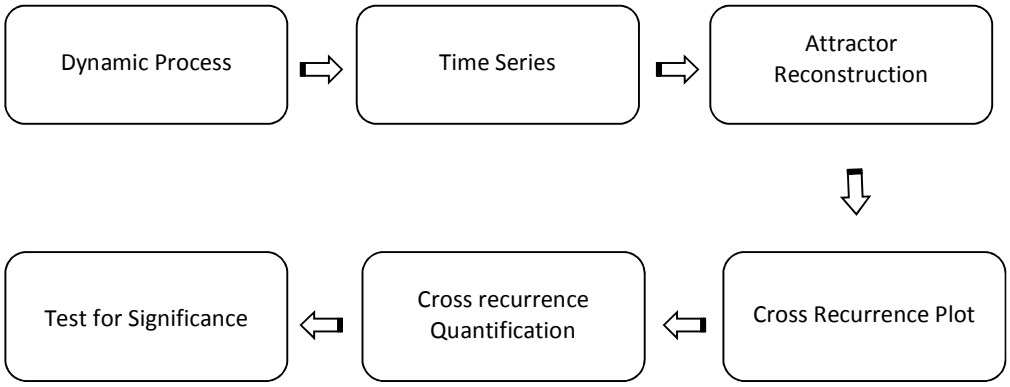

Fig. 3.6 Research Methodology

are then subjected to statistical tests for significance. The significant ones among them are taken as characteristics of the dynamics of the processes under study. Three different sets of experiments are proposed: experiment in coupled oscillator system, experiment in a lathe; set-1 and set-2. The experiment, coupled oscillator system, study the influence of coupling on the CRQA variables, whereas the lathe set-1 and set-2 are carried out to identify CRQA variables sensitive to machine tool chatter. This is to be validated later.

To obtain the spectrum of the significant CRQA variable values, in coupled oscillator system, fluids of various viscosities are used. In lathe experiment the set-1 use a stepped shaft in order to create chatter at a known location; set-2 uses a conical section having a uniform taper along the axis. The depth of cut increases gradually at

a constant rate when other important parameters speed and feed are kept constant. All cutting parameters except the depth of cut remains constant during cutting, at a certain point chatter is bound to occur. The point of starting the chatter is located using this methodology.

3.13 Wilcoxon rank-sum test

The Wilcoxon rank-sum test is a nonparametric test which is based solely on the order in which the observations from the two samples fall. The Wilcoxon test is valid for data from any distribution, whether normal or not, and is much less sensitive to outliers. It is used when comparing two related samples or repeated measurements on a single sample to assess whether their population mean ranks differ.

A general formulation assumes that:

- All the observations from both groups are independent of each other,
- The responses are ordinal (i.e. one can at least say, of any two observations, which is the greater),
- Under the null hypothesis the distributions of both groups are equal, so that the probability of an observation from one population (X) exceeding an observation from the second population (Y) equals the probability of an observation from Y exceeding an observation from X, that is, there is a symmetry between populations with respect to probability of random drawing of a larger observation.

- Under the alternative hypothesis the probability of an observation from one population (X) exceeding an observation from the second population (Y) (after exclusion of ties) is not equal to 0.5. The alternative may also be stated in terms of a one-sided test.

3.14 Summary

Recurrence is a fundamental property of dynamical systems, which can be exploited to characterize the system's behaviour in phase space. In this chapter a comprehensive overview of nonlinear time series analysis methodology, including recurrence based method is provided. The cross recurrence plot quantification analysis of time series obtained from sensor signals is done based on nonlinear dynamics concepts. The next chapter deals with the various experimental set up used to conduct the research.

4. Coupled Oscillator Experimental Setup and Data Acquisitions

In this chapter, the experimental setup, the data acquisition systems and results of the experiments on coupled oscillator are discussed.

4.1 Coupled Oscillator System

A dual-oscillator system is constructed consisting of two oscillators which were coupled via a fluid medium (Figure 4.1). It consists of an acrylic tray of size 20 cm wide, 30 cm long, 12 cm deep, driven by a stepper motor which imparts reciprocating motion. The tray is filled with a viscous fluid into which the second oscillator is submersed. The second oscillator is an aluminium rod with a plastic spindle on the top and a paddle on the bottom. The spindle is wound with a nylon string which is attached, via a series of pulleys, to a vertically suspended weight. Release of the weight and the pull of gravity caused the spindle to unwind and the rotor to spin within the viscous fluid medium of the driven tray. Magnetic sensors are placed on recording levers attached to each oscillator to reproduce their displacement positions. Displacement of each oscillator is recorded using a linear and rotary magnetic encoder with motion capture software.

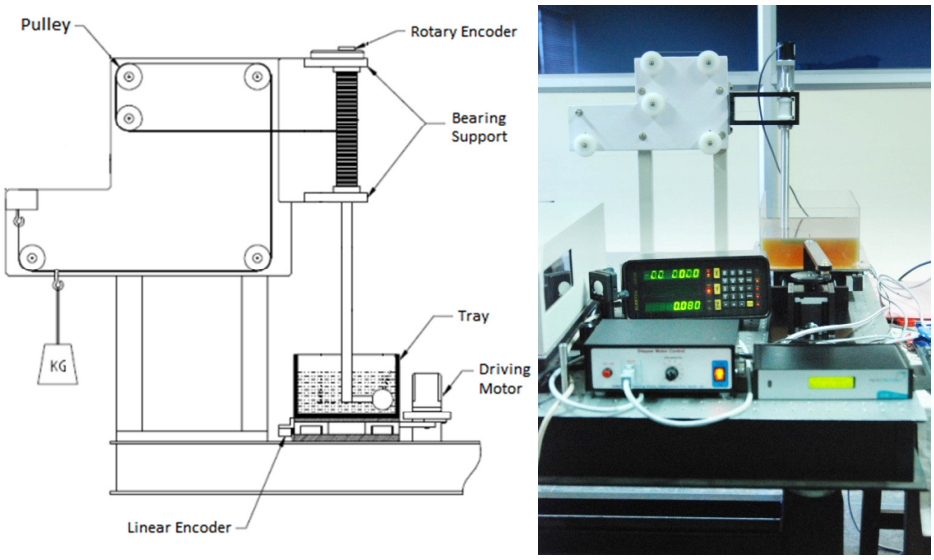

Fig. 4.1 Coupled oscillator system

4.2 Data Acquisition System

Experiments on coupled systems

During the experiments on coupled systems, two sensors are used. One is a linear encoder attached to the acrylic tray. The other one is a rotary encoder attached to the rotating shaft. The signals from both the encoders are recorded simultaneously at the same sampling rate using an EIB encoder interfacing box for analysis.

4.2.1 Linear encoder

A linear encoder is a sensor paired with a scale that encodes position. The sensor reads the scale in order to convert the encoded position into an analog signal, which can then be decoded into position. Motion can be determined by change in position over time. A 220 mm magnetic scale with slider is used. Specifications of the read head are given in table 4.1

Table 4.1 Specification of Linear encoder read head

Aluminium Die Casted Body Size: 60 x 12 x10 mm
Resolutions: 0.005 mm
Output: +5 VTTL / RS 422 / 24V line Driver
Suitable for pole pitches 5 / 2 / 2.5mm
Non - Contact Measurement
Sealed to work in dusty / oil environment

4.2.2 Rotary encoder

A rotary encoder is an electro-mechanical device that converts the angular position or motion of a shaft to an analog or digital code. Innovative make optical rotary encoder with 1000 PPR is used. Specifications are given in Table 4.2

Table 4.2 Specification of Rotary Encoder

Diameter	40mm
Shaft diameter	8 mm
Resolution	1000 PPR
Accuracy	± 15”
Output	+5V TTL square wave

4.2.3 Encoder Interfacing Box

The signals from linear and rotary encoders are recorded in a PC using a encoder interfacing box (EIB). Input signals from the linear encoder and rotary encoder are stored in the internal memory of the EIB. It is capable of recording signals at a frequency of 1 millisecond. After the completion of the test, readings are transferred to the computer. The output from the EIB is recorded to the PC through USB port. A block diagram of the RIB is given in Fig. 4.2

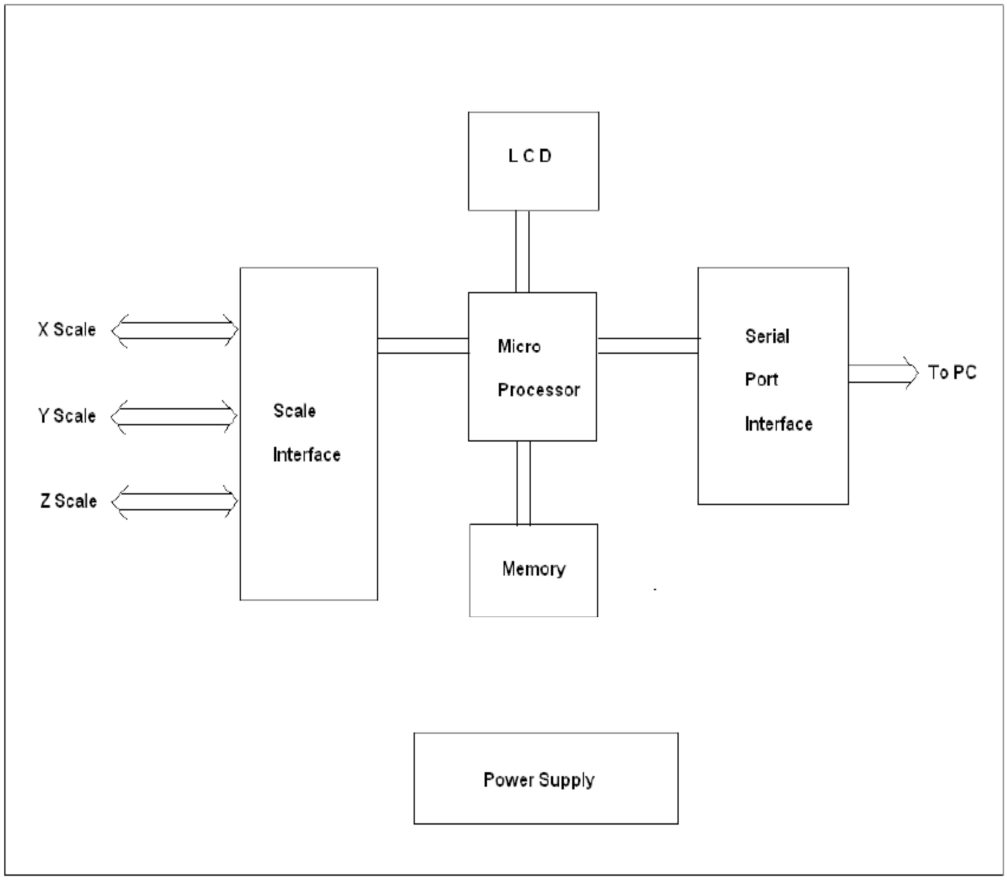

Fig. 4.2 Block diagram of encoder interface box (EIB)

4.3 Experiments and Data Acquisition

Experiments are conducted on a dual-oscillator system consisting of two oscillators which were coupled via a fluid medium. It consists of a driver (acrylic tray driven by a stepper motor which imparts reciprocating motion) and a follower (an aluminum rod with a plastic spindle on the top and a paddle on the bottom) system. The tray is filled with a viscous fluid and the second oscillator is submersed into the fluid. Displacement of each oscillator is recorded on a computer using a magnetic linear encoder and optical rotary encoder with motion capture software.

The two oscillators (driver-tray denoted by d and follower-rotor denoted by r) are coupled through viscous oils. The volume of fluid is identical in each case. The system is coupled though the viscous medium when both the tray and rotor were set into motion simultaneously. When only the rotor or tray was in motion, the system was defined as uncoupled even though the paddle is submersed in the fluid medium. The experiments are repeated with oils of differing viscosities. For each viscosity level, four trials were run for each of three couplings: driver motion with rotor motion (coupled); rotor motion without driver motion (type 1 uncoupled); driver motion without rotor motion (type 2 uncoupled). After the rotor attained the required speed, readings are taken at the rate of 1000 readings per second and a total of 7500 readings are taken per axis. To quantify relative viscosity values, the mean periods of the free-running rotor oscillator (type 1 uncoupled) were normalized to the periods of the highest viscosity. These normalized (unitless) values worked out to be as follows: 1.000 (high viscosity), 0.468 (medium viscosity), and 0.313 (low viscosity). This difference between the low viscosities became a test on the ability to detect subtle, nonlinear changes in oscillator couplings in this range.

Four sets of experiments are conducted for each fluid. The experiments are conducted for three conditions, Driver tray reciprocating, follower rotor stationary; Driver tray stationary, follower rotor rotating and both moving. From each of the experiments, 7500 data points for each axis is selected and analyzed.

4.4 Data Analysis

4.4.1 Cross Recurrence Quantification Analysis

The selection of proper embedding delay *and* embedding dimension using the AMI and FNN methods is the first step in cross recurrence analysis. The embedding dimension was set to 5 in order to capture the two-dimensional system (driver and rotor oscillators) with noise [107]. The time delay is taken as 1 to assure the highest temporal resolution between the two time signals operating at different frequencies. This is in accordance with the fact that there is no optimal lag (delay) for non-stationary systems [108]. Distances were rescaled to the maximum distance in the matrix and therefore ranged from 0% to 100%. Recurrent points are located at coordinates i, j whenever distances between specific $d_{i+m\tau}$ and $r_{j+m\tau}$ vectors fall within a predefined radius (Heaviside exclusion threshold). With low values of radius, the recurrence matrix was necessarily sparse. Since m = 5, N = 7496 for each 7500 point time series. The optimal radius was determined systematically. Because the $d_{i+m\tau}$ and $r_{j+m\tau}$ time series were dissimilar, cross recurrence plots are asymmetric across an imaginary central diagonal. Thus all CRQ plots contrasted with the ubiquitous symmetry across a prominent central diagonal for auto recurrence plots characterized by self-identity matching.

Program KRQA (109) is used to compute the elapsed time between cross recurrent points. The shortest time interval is discarded as noise, but all subsequent intervals were converted to frequency values and binned in a histogram. Bin counts were plotted as functions of frequency up to 20 Hz for alignment with the spectral plots.

The normalized time series obtained for the driver tray and driven rotor is given in Fig. 4.3.

Fig 4.4 gives the recurrence plots for the driver and the rotor. All figures are for 50 rpm speed of the driver, data recorded at 1000 Hz, and embedding dimension is taken as 2. Fig 4.4a gives the plot for low viscosity rotor, 4.4b medium viscosity rotor, 4.4c for high viscosity rotor and 4.4d for driver (tray position). By analysing the recurrence plot, it can be seen the the plot for driver motion (tray position) is almost like that of a sinusoidal wave. This is expected as the driver tray movement is periodical. The various recurrence parameters are given in the Table 4.3

Table 4.3 Recurrence parameters for the coupled oscillator

Variables	High Viscosity		Medium viscosity		Low viscosity	
	Driver	Rotor	Driver	Rotor	Driver	Rotor
Recurrence Rate (RR)	3.857	4.753	4.097	4.902	3.920	5.098
Determinism (DET)	82.570	99.439	84.400	99.550	83.434	99.659
Laminarity (LAM)	96.333	99.761	96.717	99.703	96.449	99.718
Entropy (ENT)	25.107	68.715	26.869	71.797	25.547	70.495
Traptime (TT)	5.964	6.293	6.027	6.371	5.835	6.340

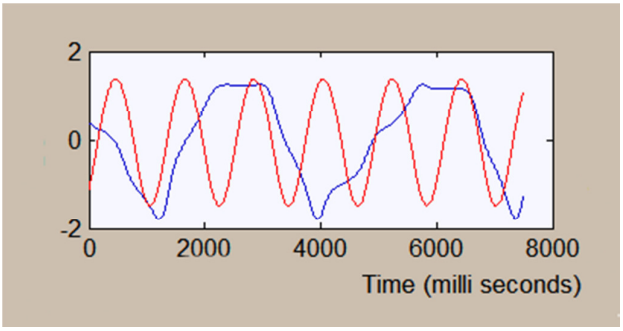

Fig 4.3 Normalised time series of driver (red) and rotor(blue)

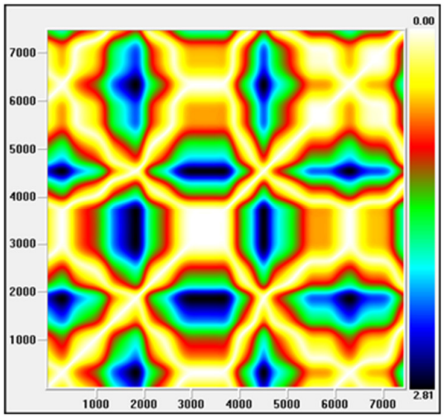

Fig. 4.4 a

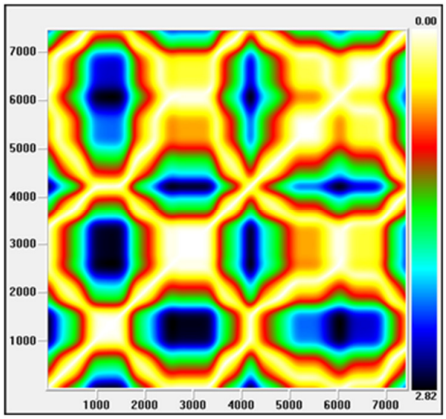

Fig. 4.4 b

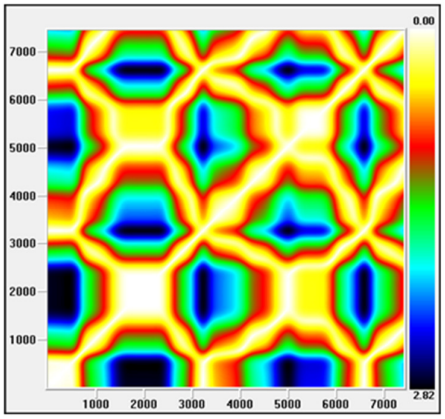

Fig. 4.4 c

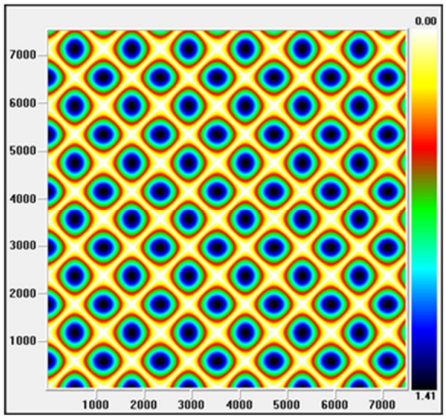

Fig. 4.4 d

Fig 4.4 Recurrence plots for the coupled oscillator.

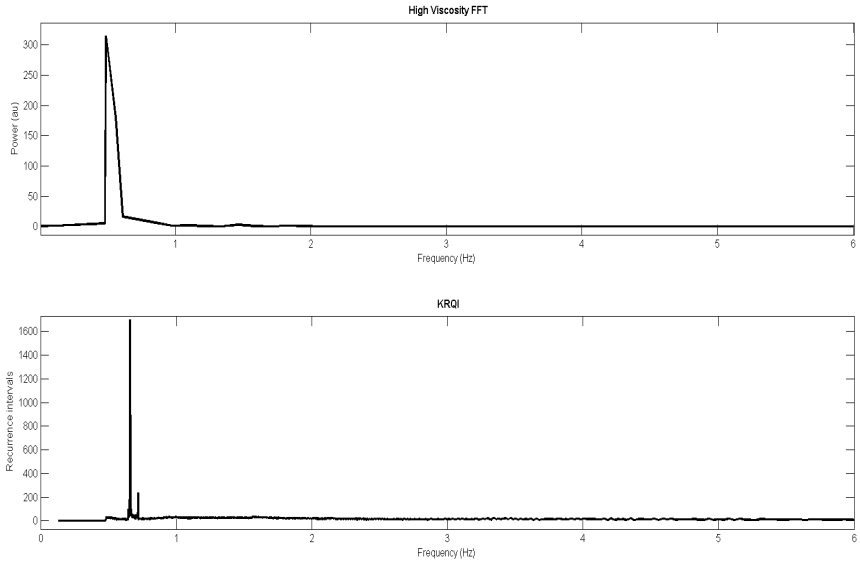

Fig. 4.5 Frequency analysis of Rotor dynamics at high viscosity - FFT (top) and CRQA (below)

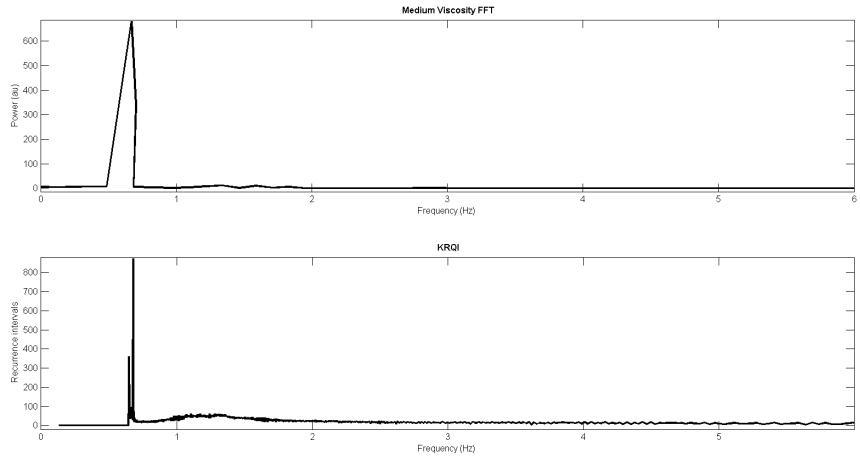

Fig. 4.6 Frequency analysis of Rotor dynamics at Medium viscosity - FFT (top) and CRQA (below)

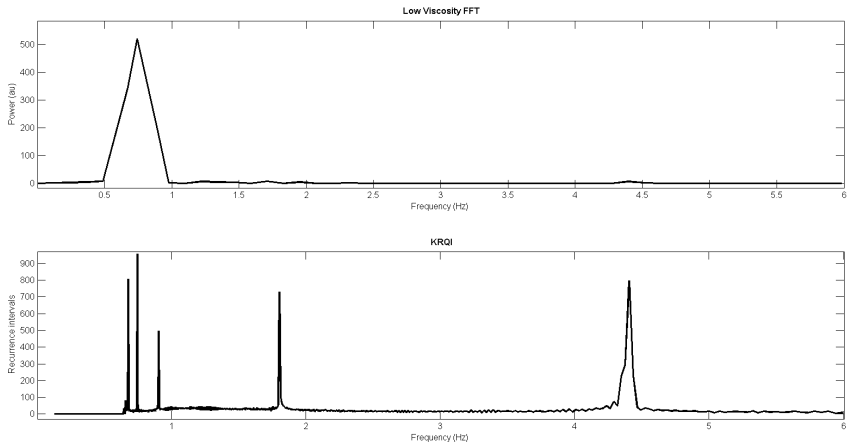

Fig. 4.7 Frequency analysis of Rotor dynamics at Low viscosity - FFT (top) and CRQA (below)

The driver tray had a fixed frequency of 0.838 Hz independent of the fluid viscosities or coupling/non-coupling interactions with the rotor oscillator. Hence the driver is stable, robust, and its oscillatory characteristics are unchanging in nature. The dependent rotor oscillator whose frequency characteristics from the linear FFT and nonlinear KRQI perspectives are shown in Fig. 4.5 to Fig. 4.7. The coupling of the two oscillators through the viscous medium caused a slowing of the rotor rotations from 0.372 Hz to 0.349 Hz to 0.297 Hz dependent upon the viscosity.

Comparing the FFT and recurrence spectra from CRQA (Fig 4.5 to 4.7), it is found that, over the frequency range of 0 Hz to 2 Hz, the frequency resolution is superior over KRQI than FFT. At frequencies from 2.0 to 6.0 Hz, cross recurrence analysis gives out more information compared to FFT. Cross recurrence analysis and FFT give essentially the same information in uncoupled situations irrespective of the fluid viscosity. But then the system is fully linear when the rotor is oscillating at

its natural frequency with no interference from the driver. Coupling of the rotor to the driver through the low and medium viscosity fluids causes a spreading out of cross recurrence analysis frequencies not clearly observed with the FFT. There are even subtle differences between the cross recurrence analysis spectra for these two viscosities that are nonetheless very close to one another. These CRQA data reveal nonlinear coupling characteristics that are completely missed by linear FFT analysis. Cross recurrence plot of the signals is given in fig 4.8. Experiment were repeated for different speed (30 rpm , 45 rpm and 50 rpm), different loads (90g, 120g, 130 g, 150 g and 230 g) and flat paddles.

An episodic test conducted on the full length of sample data sets to examine constancy of the significant CRQA variables within the whole length of data (Figure 4.9) using CRP tool box software developed by Marwan (http://www.agnld.unipotsdam.de/~marwan/toolbox/). Here an epoch is designed to have a width of 1024 data points and is made moving giving a 64 point data shift. Also, the figures show wide separations between the means of values of the recurrence variables suggesting of two distinct dynamics.

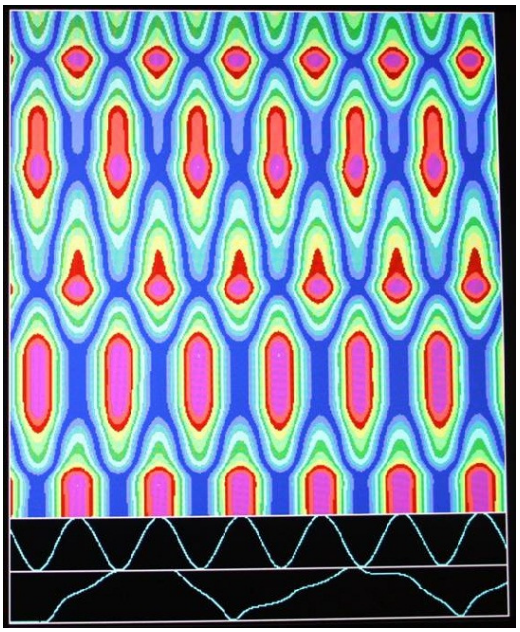

Fig. 4.8 Cross Recurrence Plot (delay 1, embedding dimension 5)

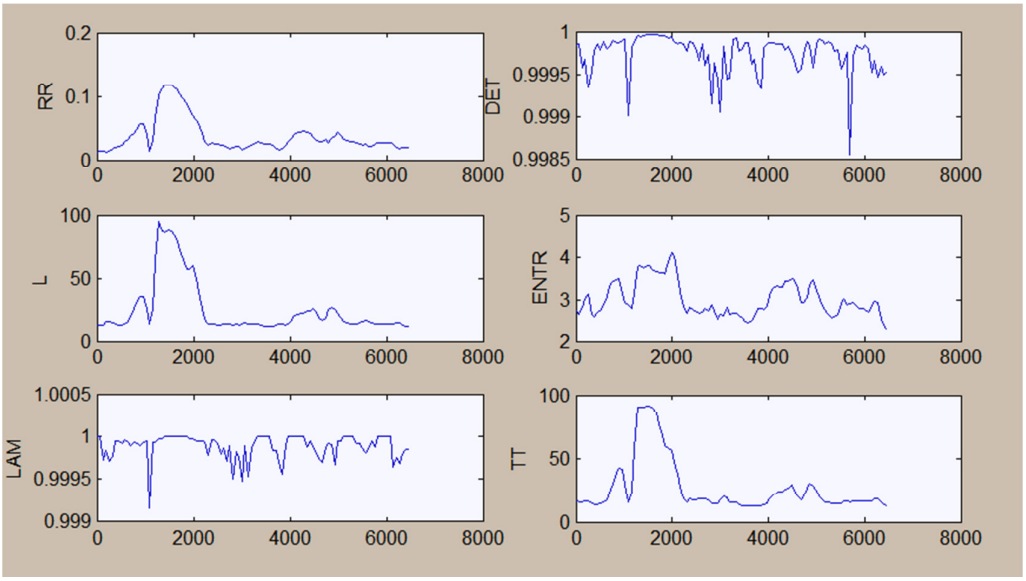

Fig. 4.9 CRQA variables of coupled oscillator

Recurrence Rate (RR), Determinism (DET), Diagonal Line length (L), Entropy (ENT), Laminarity (LAM) and Traptime (TT) from CRQA analysis. (High viscosity, 50 rpm, delay 1, embedding dimension 5)

4.4.2 Surrogate Data Test

Here, using the actual intact data, CRQA results for the coupled oscillator are compared with the CRQA results obtained after randomizing the same data points. It is found that this randomization effectively destroyed all the structures revealed under the input parameter values chosen earlier, as shown in Fig 4.10**.** For most of the CRQA variables, value is zero. Furthermore, on examination, cross recurrence plots did not resemble those for the actual intact data. Thus, it may be concluded that the results obtained under the present parameterization reflect true properties of the temporal evolution of the dynamics and contain a degree of deterministic structure. Table 4.4 shows the CRQA analysis results for surrogate data.

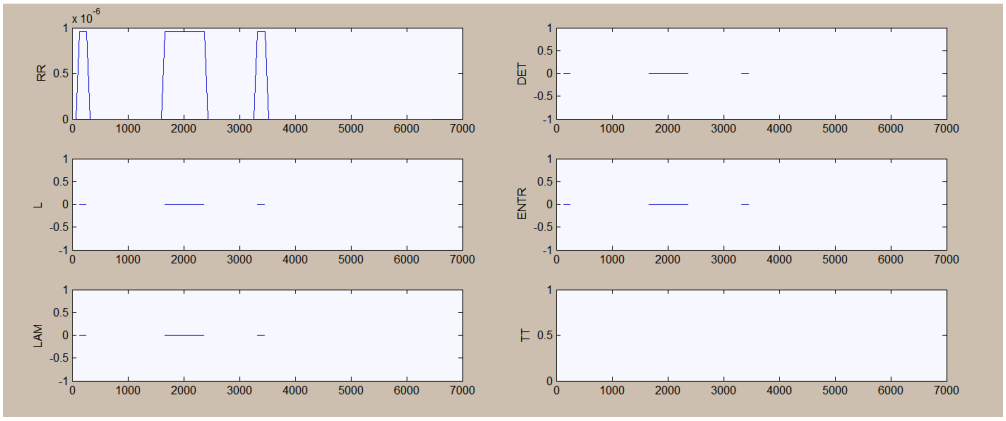

Fig. 4.10 CRQA variables for randomized data

Recurrence Rate (RR), Determinism (DET), Diagonal Line length (L), Entropy (ENT), Laminarity (LAM) and Traptime (TT) from CRQA analysis. (High viscosity, 50 rpm, delay 1, embedding dimension 5)

Table 4.4 CRQA variables for surrogate data test

	Intact data	Randomised data
Recurrence Rate (RR)	2.449	NaN
Determinism (DET)	89.863	0.000
Laminarity (LAM)	92.735	0.000
Entropy (ENT)	52.843	0.000
Traptime (TT)	6.572	0.000

4.5 Observations

1) The study revealed that the cross recurrence analysis can reveal nonlinear coupling characteristics that are completely missed by linear FFT analysis.

2) The results were repeated for different speeds (30 rpm, 45 rpm and 50 rpm), different loads (90g, 120g, 130 g, 150 g and 230 g) and flat paddle. The analysis from all these tests show similar results.

3) The surrogate data test shows that the results obtained are the true properties of the temporal evolution of the dynamics and contain a degree of deterministic structure.

4.6 Summary

In this chapter analysis of the results from various experiments in coupled oscillator set up is discussed. This forms the basis for the analysis of signals from machining to find the chatter during turning. Next chapter gives the analysis for the experiments on machine tool setup.

5. Machining Experimental setup and Data Acquisitions

In this chapter, the experimental setup for machining, the data acquisition systems, the different work pieces used and the results of the experiments are discussed.

5.1 Description of the Machine Tool

The experiments are carried out on a 3 phase, 3.7 kW, 1400-rpm PSG heavy-duty lathe using CNMG 120408 PM and CNMG 120412 PM carbide inserts with standard tool holder. The work pieces are circular in cross section and are made of various materials such as Brass, Gun Metal, Aluminium and Stainless Steel. It is held securely between a three jaw chuck and a revolving centre. The cutting factors; speed and feed per revolution and the depth of cut are varied as designed in the particular set. Various tool inserts of different nose radius are also used. During cutting, the tool overhang is set to 10 mm. No coolants or lubricants are used during the operation.

5.2 Description of the Test Specimen

Two sets of work pieces of different geometries are used in the experiments. The experiment set-1 uses a stepped shaft of length 120 mm (Figure 5.1) whereas set-2 uses a conical shaped rod of length 120 mm as shown in Figure 5.2.

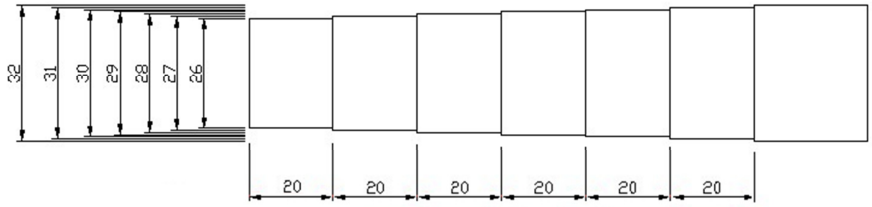

Fig. 5.1 Test specimen for Experiment Set-1

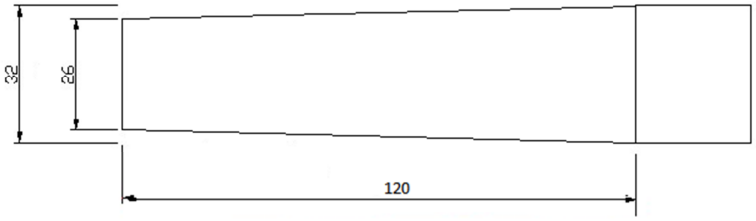

Fig. 5.2 Test specimen for Experiment Set-2

5.3 Description of the Tool Inserts

The cutting tools used in the experiments are Sandvik made CNMG 120408 PM and CNMG 120412 PM carbide inserts with standard tool holder. Both tool inserts were used in machining conical and stepped test specimens. The cutting tool insert is changed for each set of experiment so that cutting is always taken by a fresh tool. Specifications of tool insets are given in Table 5.1

Table 5.1 Specification of tool inserts

Tool insert specifications		
	CNMG 120408	CNMG 120412
Insert shape	80^0	80^0
Clearance angle	0^0	0^0
Tolerance	± 0.13 mm	± 0.13 mm
Cutting edge length	12.00 mm	12.00 mm
Thickness	4.76 mm	4.76 mm
Nose radius	0.80 mm	1.20 mm

5.4 Sensors used in machining experiments

During the machining experiments, two sensors are used. One is a lathe drive motor current sensor and the other is an accelerometer for picking tool vibrations. When used together, the sensor measurements are made simultaneously.

5.4.1 Current Sensor

Drive motor current data acquisition system uses a 3 phase line current sensor to measure the current drawn by the lathe drive motor. The sensor consists of a current transformer (CT) having an output range of ±5 volts. The analog voltage signal from the output of the CT is sent to DAC NI PCI 6221 through NI SHC68-68-EPM and SCB 68 for converting it to the digital domain. The sampling rate is fixed at 1 kHz to cover the entire frequency range of the signal. The digitized data is recorded in the PC hard drive using NI LabVIEW. A flow diagram for the sensor setup is given in Figure 5.3

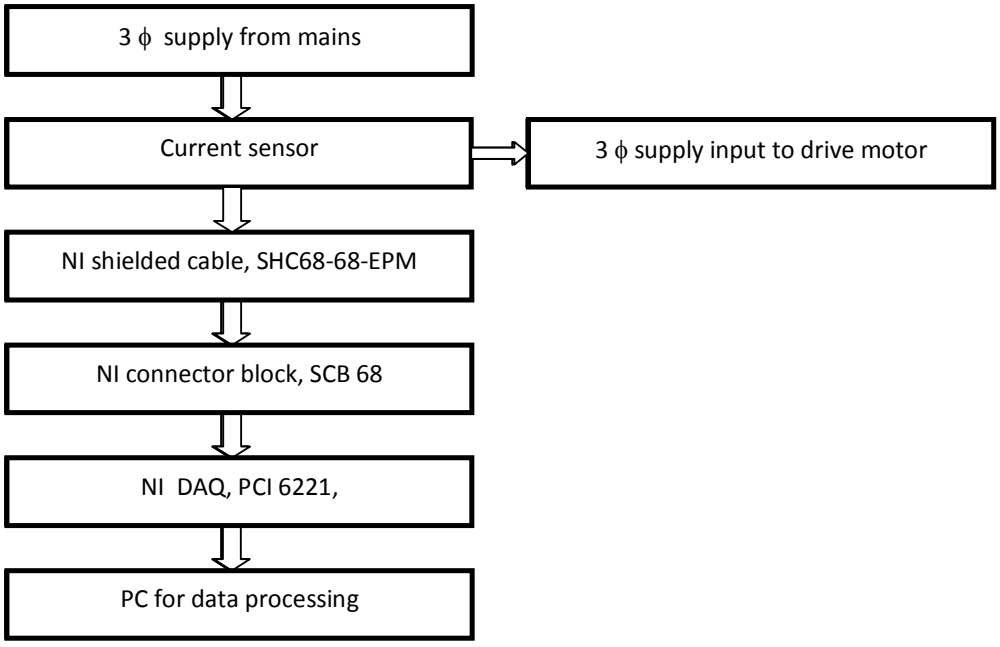

Fig. 5.3 Data acquisition flow diagram for the current sensor.

5.4.2 Vibration Sensor

To pick up the vibration of the cutting tool, an ADXL-150 accelerometer sensor is used. It is placed on the tool holder near its tail end to measure vibration in the feed direction. The resulting output voltage signal, due to vibration, is amplified and passed through a low pass filter having a cut-off frequency of 1 kHz. The sampling rate is fixed as the same as current sensor. The data acquisition system for vibration signals used a different channel of the same DAC NI PCI 6221 and similarly other peripherals along with NI LabVIEW. Figure 5.4 shows the data acquisition flow diagram for the accelerometer.

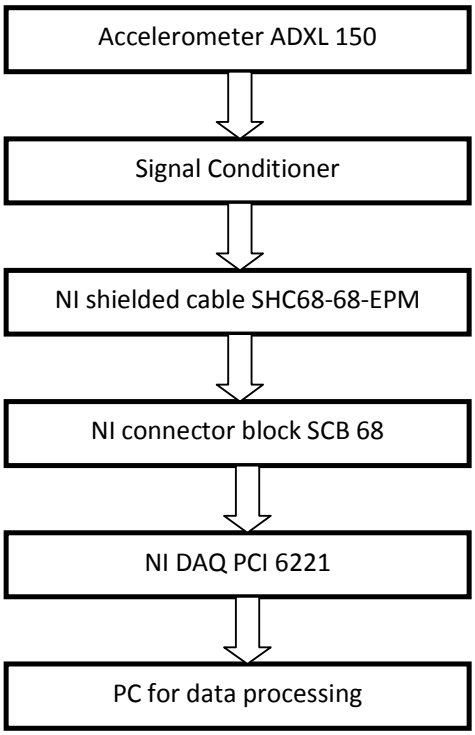

Fig. 5.4 Data acquisition flow diagram for the accelerometer

5.5 Description of the Data Acquisition System-NI components

- DAC NI PCI 6221

Data acquisition card with two 16-bit analog outputs (833 kS/s); 24 digital I/O; 32-bit counters

- SHC68-68-EPM

This cable is designed to work with NI PCI 6221. It includes separate digital and analog sections, individually shielded twisted pairs for analog inputs, individually shielded analog outputs, and twisted pairs for critical digital I/O.

- SCB 68

Noise rejecting, shielded I/O connector block for NI PCI 6221 with 68-Pin Connectors

5.6 Description of the Accelerometer ADXL 150

A transducer converts the mechanical vibrations of the lathe cutting tool into proportional electrical signals. An acceleration sensitive transducer, called accelerometers is selected here. An accelerometer is an electromechanical transducer which produces at its output terminals, a voltage or charge that is proportional to the acceleration to which it is subjected. The piezoelectric elements within the accelerometer have the property of producing an electrical charge which is directly proportional to the strain and hence to the applied force when loaded either in tension, compression or shear. For frequencies lying well under the resonant frequency of the assembly, the acceleration of the masses will be the same as the acceleration of the base, and the output signal level will be proportional to the acceleration to which the accelerometer is subjected.

The accelerometers are smaller in terms of relative mass than velocity pickups and that their frequency and dynamic ranges are significantly wider, even after integration to velocity. A supplementary factor which emphasizes the benefits of accelerometers is that an accelerometer signal can be effortlessly and suitably integrated electronically to get velocity and displacement.

The ADXL 150 is a third generation ±50g surface micro accelerometer (Figure 5.5). It offers lower noise, wider dynamic range, reduced power consumption and improved zero g bias drift. It is a single axis accelerometer with signal conditioning on a single monolithic IC. Power consumption is modest at 1.8mA per axis. The ADXL 150 is available in a hermetic 14-lead surface mount cerpac package specified over the 0^{o} to $+70^{o}$ C commercial and -400^{o}C to $+85^{o}$C industrial temperature ranges. Generally used in Vibration measurement, Shock detection, Machine condition monitoring, Fleet monitoring and Event recording.

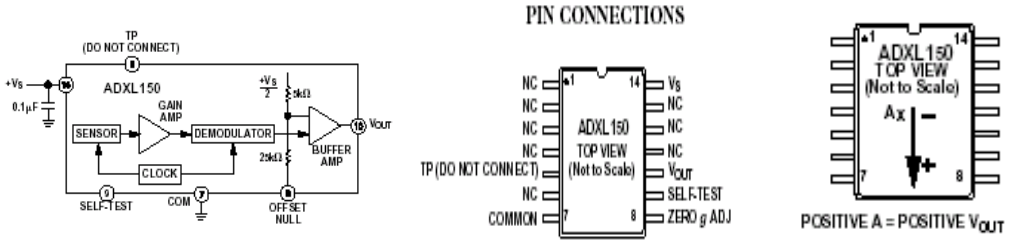

Functional block diagram | Pin connections | Sensitive axis orientation

Fig. 5.5 ADXL 150 accelerometer details

Figure 5.6 shows the experimental setup for the data acquisition. The current sensor and the signal conditioner for the vibration signals are shown. The conditioned signals from the vibration sensor and current sensor are coming to the connector block. From there a sheathed cable takes the data to the DAQ card in the personal computer. It is recorded in the hard disk with the help of the labview software.

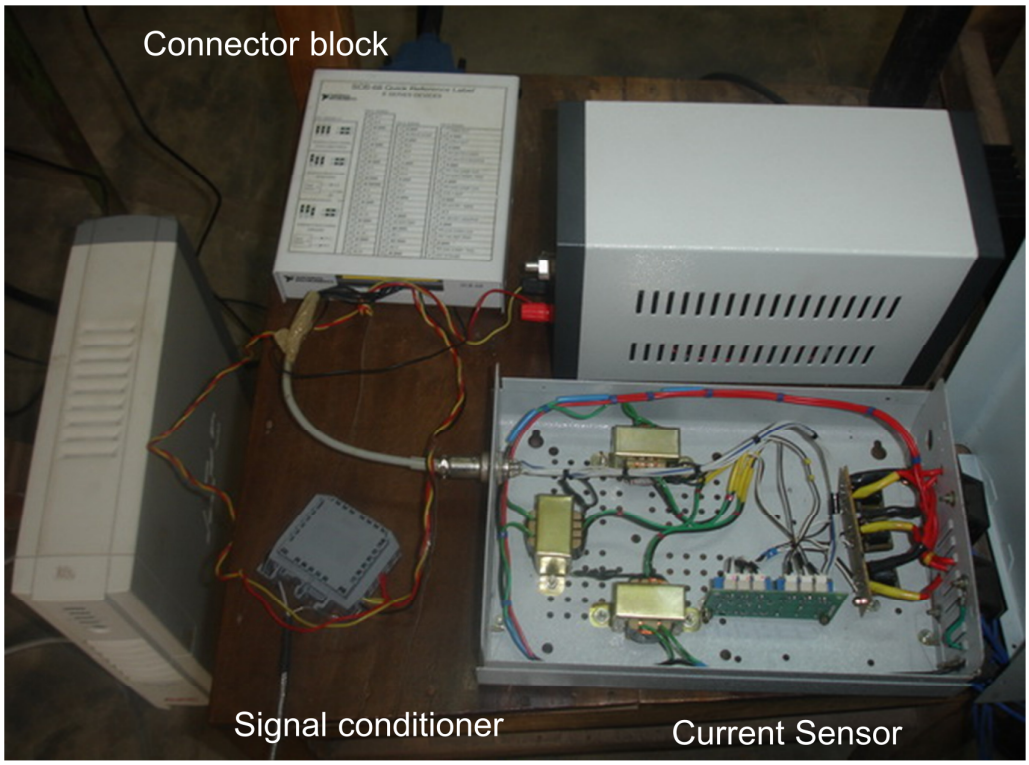

Figure 5.6 Experimental setup for data acquisition

5.7 Multiple regression modelling

Basic aim of any manufacturing process is to produce high quality products at a low cost. High speed, feed and depth of cut are used to achieve high metal removal rate but this leads to surface roughness and chatter. Surface finish of the machined surface is an important indicator of chatter. To determine the dependency of surface roughness on vibration and major machining parameters like speed, feed and depth of cut, multiple regression modelling is done. This methodology is used for determining the most significant parameter for use in surface roughness prediction in turning operations. Tests were conducted at two different speeds (360 and 560 rpm), three feed rates (0.06, 0.08 and 0.1 mm/rev), six different depths of cut. The vibration signals were analyzed by transforming them into absolute values

of amplitude. The parameters and the results of the experimental runs, including surface roughness measurements and mean vibration amplitudes, are shown in Table 5.2

Table 5.2 Factors and responses Data

Run	Speed RPM	Feed mm/rev	Depth of cut mm	Roughness Ra(microns)	V Vibration amplitude
1	360	0.06	0.5	1.88	0.050465
2	360	0.06	1.0	3.47	0.155285
3	360	0.06	1.5	2.00	0.294262
4	360	0.06	2.0	9.59	0.340847
5	360	0.06	2.5	15.12	0.366432
6	360	0.06	3.0	17.88	0.356699
7	360	0.08	0.5	7.32	0.093459
8	360	0.08	1.0	6.96	0.071048
9	360	0.08	1.5	6.50	0.13961
10	360	0.08	2.0	4.36	0.161439
11	360	0.08	2.5	5.19	0.14654
12	360	0.08	3.0	5.30	0.128026

Run	Speed RPM	Feed mm/rev	Depth of cut mm	Roughness Ra(microns)	V Vibration amplitude
13	360	0.10	0.5	3.10	0.007207
14	360	0.10	1.0	7.28	0.023983
15	360	0.10	1.5	6.25	0.056492
16	360	0.10	2.0	6.08	0.068671
17	360	0.10	2.5	10.42	0.058858
18	360	0.10	3.0	3.58	0.058837
19	560	0.06	0.5	2.59	0.027802
20	560	0.06	1.0	4.39	0.041515
21	560	0.06	1.5	3.48	0.313158
22	560	0.06	2.0	3.27	0.307935
23	560	0.06	2.5	3.72	0.409473
24	560	0.06	3.0	4.21	0.396234
25	560	0.08	0.5	1.71	0.019233
26	560	0.08	1.0	2.52	0.052882
27	560	0.08	1.5	3.63	0.248893
28	560	0.08	2.0	3.97	0.270017
29	560	0.08	2.5	3.63	0.198849
30	560	0.08	3.0	2.21	0.153526
31	560	0.10	0.5	4.40	0.084869
32	560	0.10	1.0	6.43	0.258318
33	560	0.10	1.5	1.99	0.335867
34	560	0.10	2.0	1.70	0.3714
35	560	0.10	2.5	3.77	0.390639
36	560	0.10	3.0	3.26	0.453582

The data is then used to create a prediction model based on multiple regression. In order to minimize the model, both informal and statistical analyses were performed on these data to determine the minimum and most significant turning parameters and vibration components. Minimizing the model and using the simplest terms would therefore begin with attempting to use the basic parameters and vibration components—feed rate, spindle speed, depth of cut, and the vibration signals.

An initial analysis was performed to determine the Pearson correlations between the factors and response. As seen in Table 5.2, all of the factors except spindle speed and depth of cut were found to have significant correlation coefficients. Therefore, it is likely that spindle speed and depth of cut do not have a significant effect on surface roughness.

Table 5.3 Pearson correlations between factors and responses

Predictor	Coef	SE Coef	T	P
Constant	13.496	3.546	3.81	0.001
S	-0.02014	0.00556	-3.62	0.701
F	-16.04	31.95	-0.5	0.009
D	0.5289	0.7365	0.72	0.478
V	6.327	5.035	1.26	0.218

The coefficients calculated with the regression analysis result in the following predictive equation:

$$R = \beta_0 + \beta_S S + \beta_F F + \beta_D D + \beta_V V \quad (1)$$

R – Surface Roughness F – Feed Rate

S – Spindle speed D – Depth of cut

V – Vibration Amplitude β – Linear constants

Null hypothesis is that none of the variables are significant.

Table 5.4 Analysis of variance

Analysis of Variance

Source	DF	SS	MS	F	P
Regression	4	157.62	39.405	4.4	0.006
Residual Error	31	277.71	8.958		
Total	35	435.329			

A small p-value rejects the null hypothesis that none of the independent variables are significant.

Multiple regression model is:

$$R = 13.5 - 0.0201 S - 16.0 F + 0.529 D + 6.33 V \quad (2)$$

From the equation (2) it can be seen that the influential parameter is feed rate and then vibration. A strong linear relationship among the parameters (feed rate and vibration) and the response (surface roughness) is found using multiple regression and ANOVA. This test of significance shows that the cutting parameters are significant independent variables for predicting roughness.

Chatter results from unwanted vibration of the machine tool, workpiece, tool system. As chatter has many detrimental effects, it is desirable to avoid chatter at all costs.

5.8 Experimental setup for detection of chatter

CRQA variables can intimately portray dynamical behaviour of the cutting process under conditions of chatter than any other measures of nonlinearity which is rather weighed down by the noise and the non-stationarity of data. This leads us to the supposition that the trends exhibited by CRQA variables during chatter free-to-chatter regimes of cutting will be identical under any conditions or configurations of operation and therefore can be taken as characteristics of the dynamic response that can convey the chatter conditions reliably. As a result this study explores applicability of the CRQA methodology in detecting the transition from chatter free to chatter cutting during turning process.

The experiment is conducted in two parts here. In one part the stepped shaft is used as the workpiece in an attempt to identify the significant CRQA variables responding to machine tool chatter. The second part is conducted to validate the nature of variation of the identified sensitive CRQA variables when the cutting changes from chatter free to chatter in an actual situation.

5.8.1 Experiment Set 1

Sensitivity of the significant CRQA variables to cutting dynamics during chatter free and chatter situations are examined here for the stepped shaft .

5.8.1.1 Experiments and Data Acquisition

Various work piece materials (Brass, Copper, Gun metal, AISI 1025 carbon steel and Stainless steel) of two different geometries are used for the experiment. The results for the AISI 1025 carbon steel are presented. The test specimen in the present study is a rod of 32 mm diameter, converted into stepped work piece with small end diameter of 26 mm and the larger end diameter of 31 mm which has 120 mm axial length as shown in Figure 5.2. The cutting has been carried out in a heavy duty lathe of PSG make. The work involves reducing the stepped section into a rod of 25 mm uniform diameter in a single pass of the cutting tool. A CNMG 120408PM cutting tool with standard tool holder is used for this purpose. A feed rate of 0.1 mm/rev. at 560 rpm are set as the fixed cutting parameters whereas the depth of cut increases along the axis of the specimen owing to the geometry of the section; the depth of cut varying from 0.5 mm to a maximum of 3 mm at the 120mm axial distance from the smaller end. The experiment is repeated for speed of 360 rpm and for feed rate of 0.08 mm/rev. and 0.06 mm/rev. and also with CNMG 120412 PM cutting tool.

The two regimes of cutting; the chatter free and the chatter cutting are created by performing turning on a workpiece consisting of a stepped shaft. This particular design ensured that the cutting have been chatter free for the first part where the depth of cut have been low and when it suddenly increases the condition changes into chatter cutting. Several trials of experiments are carried out by varying the speed, feed and the cutting tool.

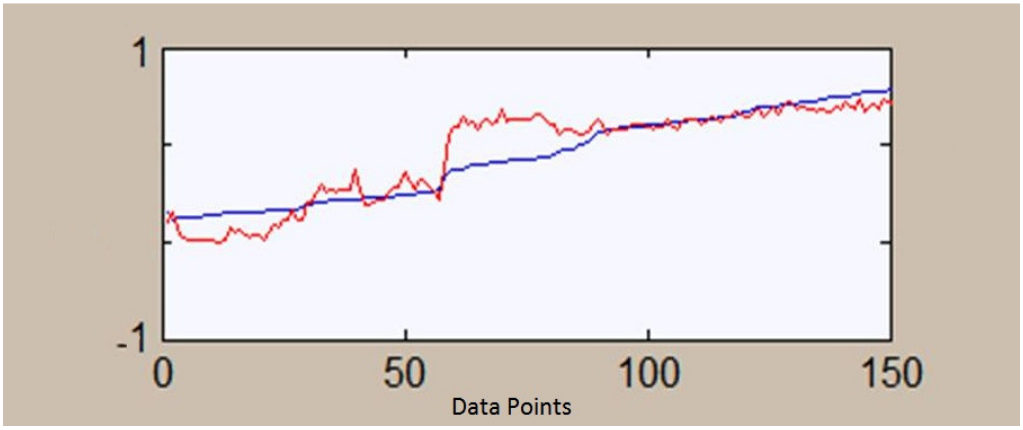

Fig. 5.7 Normalized Time series chart of input values velocity (red line) and power (blue line)

A typical time series is shown in Figure 5.7. This data set represents the normalized velocity and power values.

5.8.1.2 Data Analysis

The CRQA of the experimental time series is performed after determining the phase space reconstruction parameters τ and m by using AMI and FNN methods. The threshold ε is chosen by analyzing the measure of recurrence point density as percentage of maximum distance. The obtained values are shown in Table 5.5 and the cross recurrence plot is shown in fig. 5.8

Table 5.5 CRQA input parameters for AISI 1025 carbon steel time series

Power and Vibration Sensor Data			
Parameters	τ	m	ε
value	1	8	1.5

In the cross recurrence quantification analysis the significant CRQA variables are computed for each epoch and presented in Figure 5.8. An epoch is designed to have a width of 64 data points and is made moving by giving a 1 point data shift. Studying variations in the CRQA variable values with changing epochs, these plots demonstrate heavy fluctuations in all CRQA variable values at epoch number 32, without showing any definite trend. Beyond the epoch 61 the volatility appears to settle down. It may be noted that, the change in depth of cut that has increased to 2.0 mm at the 20 mm step causes the operation to chatter cutting. This step is lying near to epoch 32 in the analysis. Beyond this point the chatter conditions should prevail owing to the higher depth of cut where the speed and feed rates still remains the same as in chatter free cutting region, i.e. before that of the step. Moreover, it has already been reported that, in turning, at the transition from chatter-free cutting to chatter, a significant increase of determinism is usually observed [110,111]. Further, it is known that onset of chatter represents a transition from high-dimensional to low-dimensional dynamics. These findings come in support for the varying trends seen in CRQA variables.

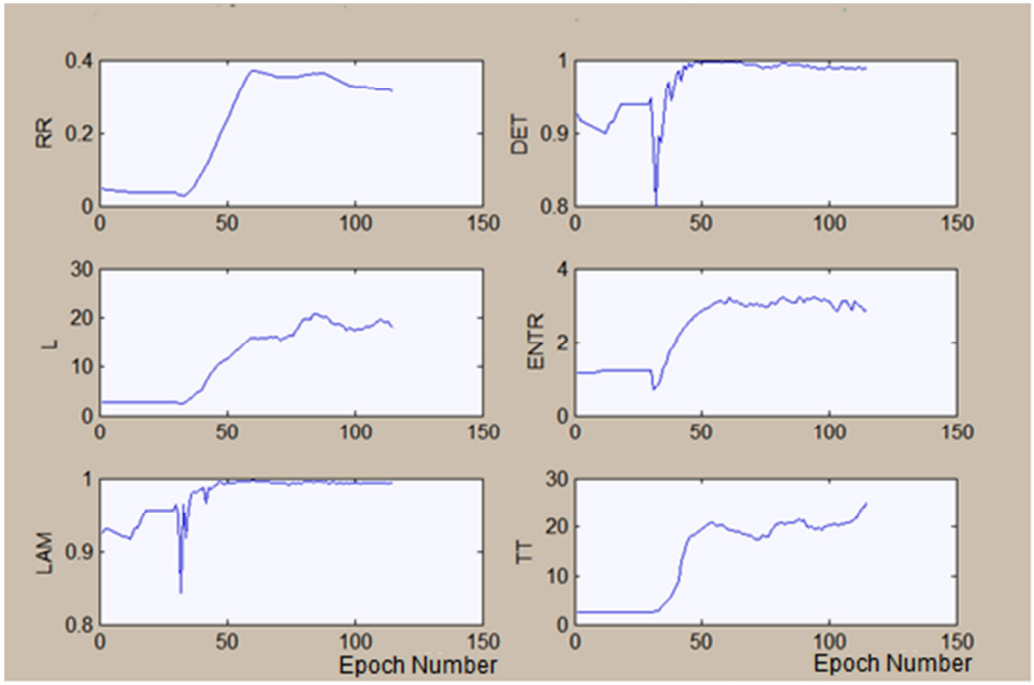

Fig. 5.8 CRQA variables for AISI 1025 carbon steel – stepped shaft

Recurrence Rate (RR), Determinism (DET), Diagonal Line length (L), Entropy (ENT), Laminarity (LAM) and Traptime (TT) from CRQA analysis.
(Speed 560 rpm, feed 0.08 mm/rev, delay 1, embedding dimension 8)

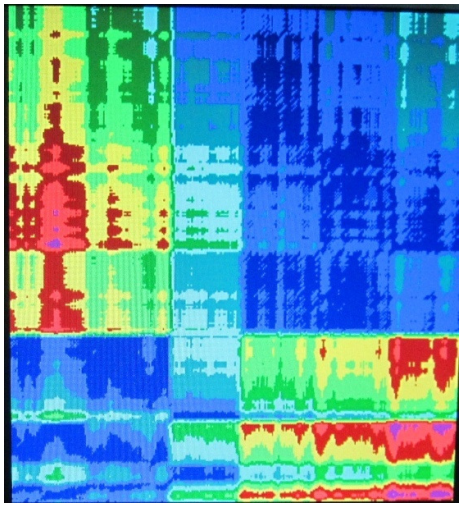

Fig. 5.9 Cross recurrence plot of Velocity and power
(AISI 1025 carbon steel)
(Dimension: 8, Delay: 1, fixed distance Euclidean norm)

At the onset of chatter the RR, ENT and TT values, in general, shows an uptrend whereas DET and LAM shows a downward trend indicating that these CRQA variable are sensitive to chatter vibrations during cutting. The plot could thus vividly indicate the two regions of cutting. Figure 5.9 gives the cross recurrence plot of the velocity and power for the machining of AISI 1025 carbon steel.

5.8.2 Experiment Set 2

Sensitivity of the significant CRQA variables to cutting dynamics during chatter free and chatter situations are examined here for the conical shaft .

5.8.2.1 Experiments and Data Acquisition

In order to verify the sensitivity of the percent determinism to chatter as it sets in or during its occurrences, several experiments are conducted using a cylindrical work piece of continuously varying cross-section (Figure 5.3) and captured the sensor signals when the cutting is taking place. The work piece has an operating length of 120 mm. The diameters are 26 mm at one end and increased with a constant taper to 32 mm at the 120 mm length giving it a truncated conical shape. During experiments the speed (560 rpm), feed (0.06 mm per revolution) are maintained constant while the depth of cut is increased slowly but steadily from 1.0 mm to 3.0 mm. This is accomplished due to the shape of the work piece. This geometry is similar to the one used by Grabec [112] in his experiments reporting the capability of coarse grained entropy rate of the time series to detect onset of chatter. The experiments are repeated for 360 rpm speed and feed rate of 0.08 mm/rev and 0.1

mm/rev. The sensor signals are recorded as Part-2 experimental time series for analysis.

5.8.2.2 Data Analysis

The embedding parameters for Part-2 experimental time series and its threshold radius are found out as before and their values are listed in Table 5.6. The CRQA outputs on the time series is carried out epoch by epoch with constant input parameters. The fluctuations in values of the various CRQA variables from the episodic test is shown in Figure 5.10 and the corresponding CRP is given in Figure 5.11

Table 5.6 CRQA input parameters for AISI 1025 carbon steel time series

Power and Vibration Sensor Data			
Parameters	τ	m	ε
value	1	8	1.4

Most of the CRQA parameters show a sharp variation at epoch no. 140. It is seen that this corresponds to a distance of 70 mm away from the tip. The percent determinism remains constant up to a depth of cut of 3.5 mm and afterwards it is seen a sudden decrease at a rapid rate. The plot data set that is fitted with a cubic spline exhibits this behaviour.

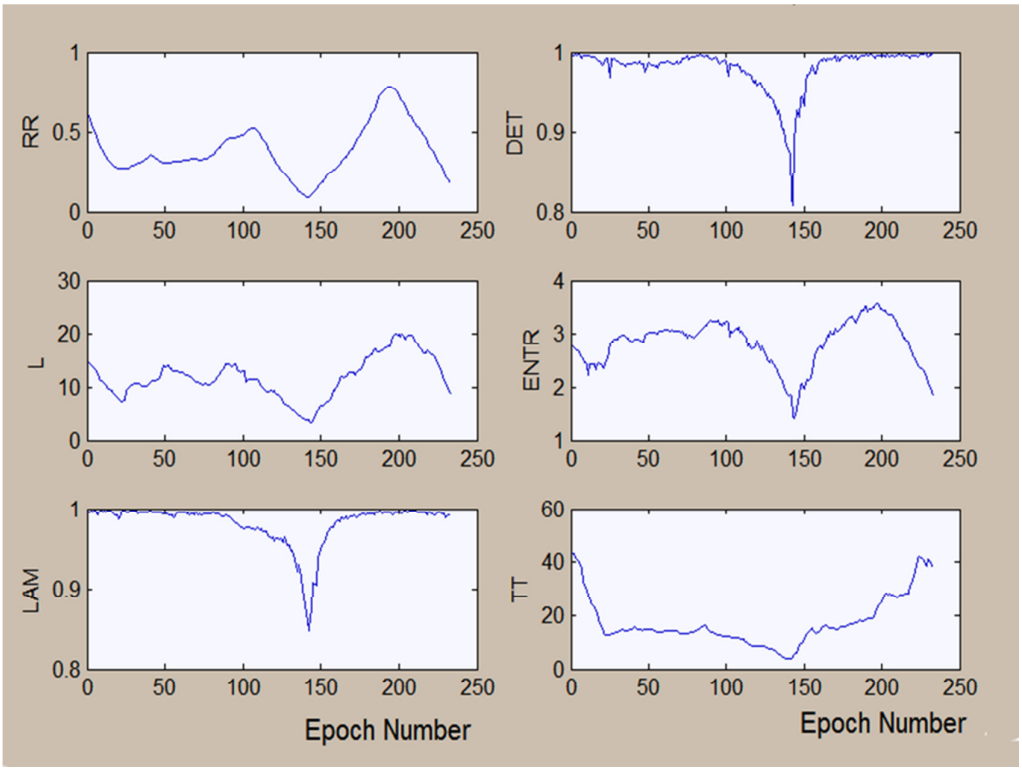

Fig. 5.10 CRQA variables AISI 1025 carbon steel (Conical shaft)

Recurrence Rate (RR), Determinism (DET), Diagonal Line length (L), Entropy (ENT), Laminarity (LAM) and Traptime (TT) from CRQA analysis.
(speed 360 rpm, feed 0.06 mm/rev, delay 1, embedding dimension 8)

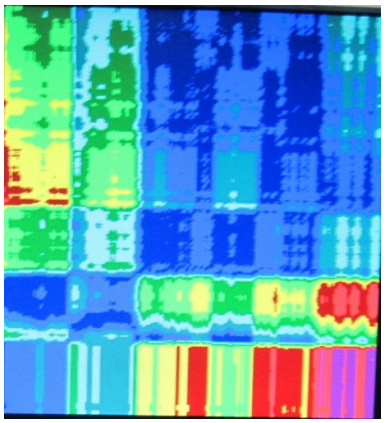

Fig. 5.11 Cross recurrence plot of Velocity and power
(AISI 1025 carbon steel)
(Dimension: 8, Delay: 1, fixed distance Euclidean norm)

Comparing with the pattern in Figure 5.8, this upward trend that begins at 35 mm can be attributed to chatter. The other two CRQA variables, %REC and ENT, also show this trend. Different trial samples of Part-2 experimental time series also gave exactly similar trends corroborating the sensitivity of CRQA variables to chatter.

In the cross recurrence quantification analysis of Brass, variations in the CRQA variable values with changing epochs, demonstrate heavy fluctuations in all CRQA variable values at epoch number 110 (Figure 5.12). Beyond the epoch 110 the volatility appears to settle down. It may be noted that, the change in depth of cut that has increased causes the operation to chatter cutting. This point is lying near to epoch 110 in the analysis which is 47.15 mm away from the tip of the work piece. Beyond this point the chatter conditions should prevail owing to the higher depth of cut. The CR Plot is given in Figure 5.13

In the cross recurrence quantification analysis of AISI 201 stainless steel (Figure 5.14), drastic variations in the CRQA variable values are seen at epoch number 145 which is 30.55 mm away from one end of the work piece. The change in depth of cut causes the operation to chatter cutting. Beyond this point the chatter conditions should prevail owing to the higher depth of cut. The cross recurrence plot is given in figure 5.15.

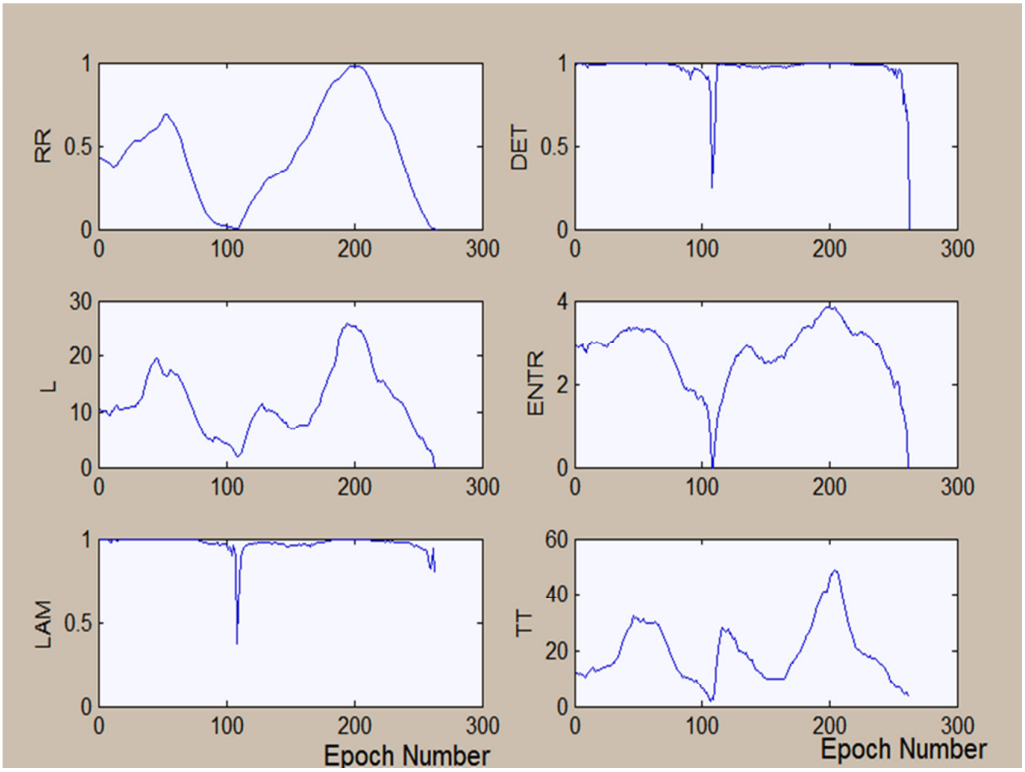

Fig. 5.12 CRQA variables (Brass)

Recurrence Rate (RR), Determinism (DET), Diagonal Line length (L), Entropy (ENT), Laminarity (LAM) and Traptime (TT) from CRQA analysis. (delay 1, embedding dimension 8)

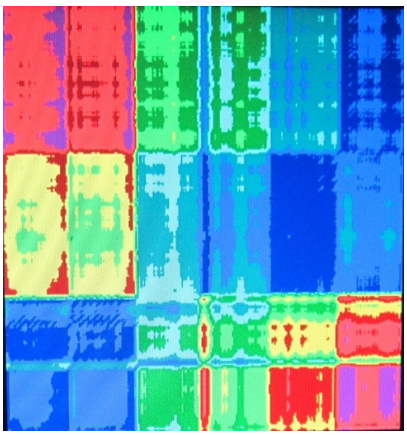

Fig. 5.13 Cross recurrence plot of Velocity and power (Brass)
(Dimension: 8, Delay: 1, fixed distance Euclidean norm)

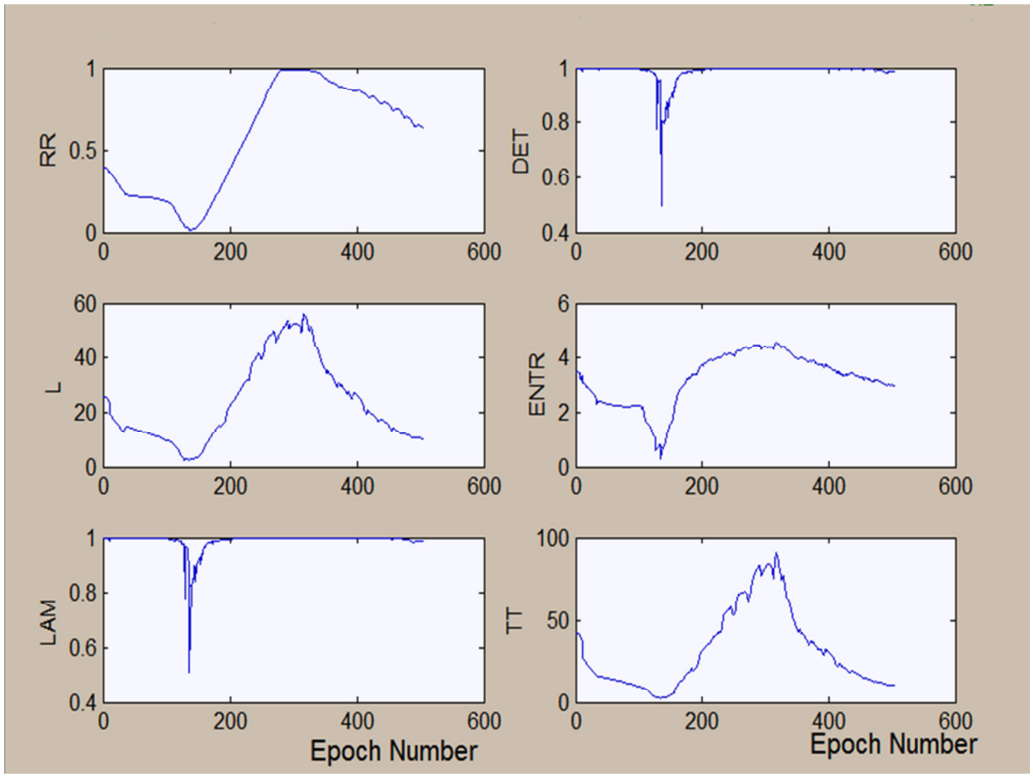

Fig. 5.14 CRQA variables (AISI 201 Stainless Steel)
Recurrence Rate (RR), Determinism (DET), Diagonal Line length (L), Entropy (ENT), Laminarity (LAM) and Traptime (TT) from CRQA analysis. (delay 1, embedding dimension 8)

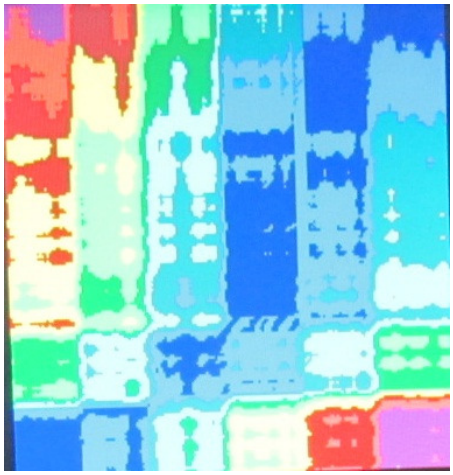

Fig. 5.15 Cross recurrence plot of Velocity and power (AISI 201 Stainless Steel)
(Dimension: 8, Delay: 1, fixed distance Euclidean norm)

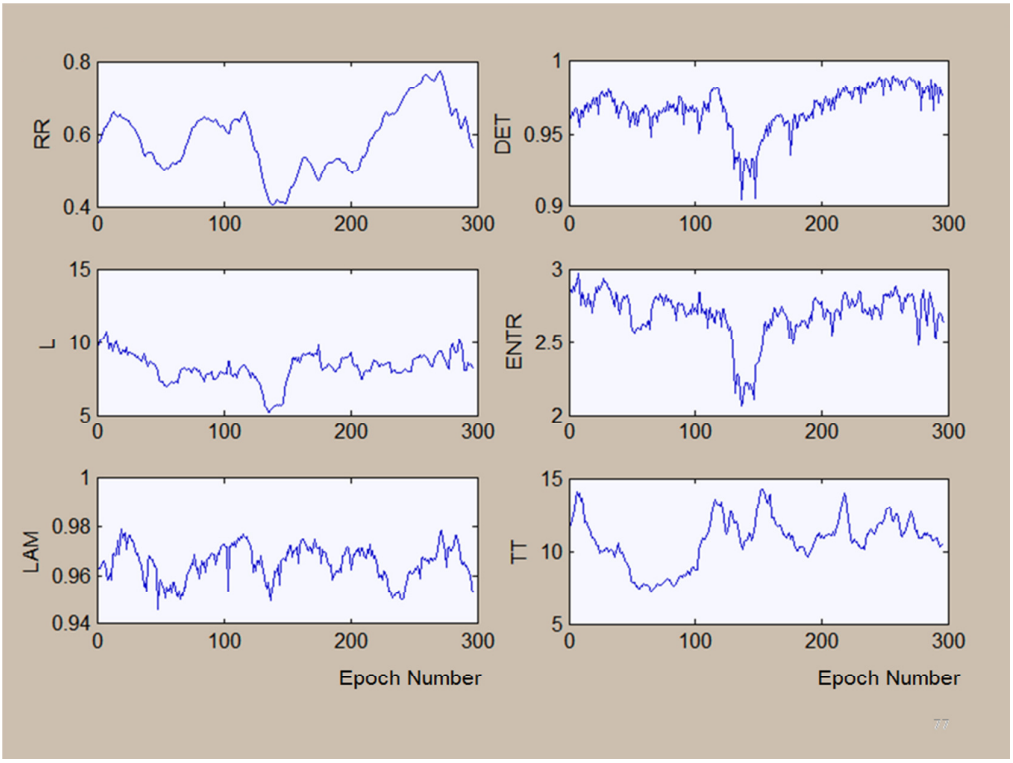

Fig. 5.16 CRQA variables (Gun metal)
Recurrence Rate (RR), Determinism (DET), Diagonal Line length (L), Entropy (ENT), Laminarity (LAM) and Traptime (TT) from CRQA analysis. (delay 1, embedding dimension 8, speed 360 rpm, feed 0.08 mm/rev)

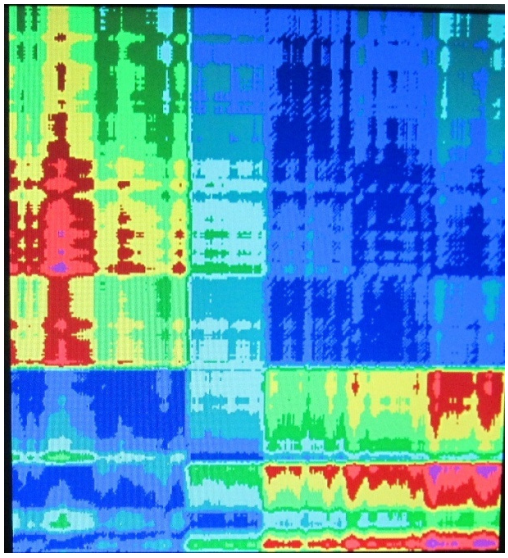

Fig. 5.17 Cross recurrence plot of Velocity and power (Gun metal)
(Dimension: 8, Delay: 1, fixed distance Euclidean norm)

In the cross recurrence quantification analysis of gun metal (Fig 5.16), the CRQA variable values show a definite trend at about the epoch number 140. This point is 54.9 mm away from the tip of the workpiece. Recurrence rate, determinism and entropy show a definite dip at the same point. On verification, it is seen that the chatter has started at this point. This transition in dynamics is verified from the variation in waviness of the surface. CRP is given in figure 5.17

5.9 Analysis based on Permutation entropy

Permutation entropy (PE) gives quantitative information about the complexity of a time series. The variation of PE as a function of time can effectively indicate dynamical change. With the onset of chatter, strongly synchronized vibrations build up and these chatter vibrations present itself in the dynamics as a lowering of dimensionality of the system and thereby an increase in the predictability of the system dynamics. Computation of PE is based on comparison of neighbouring values in the time series of any dynamical variable of a system [113].

Variation in surface texture from chatter free to chatter regime of the machined workpiece is analysed using PE of the speckle pattern acquired using speckle photographic method. The laser speckle pattern is recorded using Charge Coupled Device (CCD) camera and the gray level intensity histogram [114] derived from it is used for further analysis of surface texture. PE of the mean calculated from the intensity histogram is effective in revealing the change in surface texture produced by chatter vibrations.

5.9.1 Speckle Analysis of Machined surface

The two regimes of cutting; the chatter free and the chatter cutting are created by performing turning on the designed conical work piece. For and up to some depth of cut the cutting have been chatter-free and for all depths beyond this point it is highly likely that the condition have been chatter-cutting.

PE analysis is applied to the time series constructed using information contained in speckle images of machined surface for chatter detection in turning operation. Variations in the roughness of machined surface created by virtue of chatter, manifests as changes in the statistical properties of speckle images of the surface when examined frame by frame along the axis of the machined part. A significant parameter of such images, the frame wise average intensity value is extracted separately and arranged in sequence for constructing the time series. Since this time series is found to be non-stationary in nature and due to the fact that the turning operation is low dimensional chaotic, the nonlinear time series analysis methodology of PE is used for analyzing the time series.

The conical work piece machined straight (Figure 5.18) from earlier experiment is used for the speckle analysis. With the continuous increase in depth of cut, a progressive reduction in surface finish is expected due to increase in chip thickness. Keeping the spindle speed and feed rate constant the chatter is to begin at some increased depth of cut or chip thickness. When the chatter has begun, a drastic reduction in surface finish must result due to non-uniform chip thickness. The

variations in the surface finish are recorded in speckle images captured in sequence from point to point along the axis of the rod.

Speckle photographs of the machined surface are taken using Helium -Neon laser with a maximum of 10 mW power out at 633nm. A spatial filter lens of 10mm focal length and 25μ pinhole size were used in conjunction with it. The spatial filter output was collimated using an objective lens of 5cm focal length. The laser beam after filtering and collimation fall over the machined surface at an angle of 45 degrees. The incident light which scatters off the surface has been focused using a lens of focal length 10cm and the resulting subjective speckle pattern was recorded.

A Sony make Charge Coupled Device (CCD) array of VGA type, 1/3 inch, with 8 bit mono recording and with 7 micrometer pixel size was used in the recording. The exposure and the gain of the CCD were adjusted to ensure that the recorded intensity lies well below the saturation value. For obtaining the maximum contrast of speckle pattern the position of the focusing lens and CCD array were adjusted.

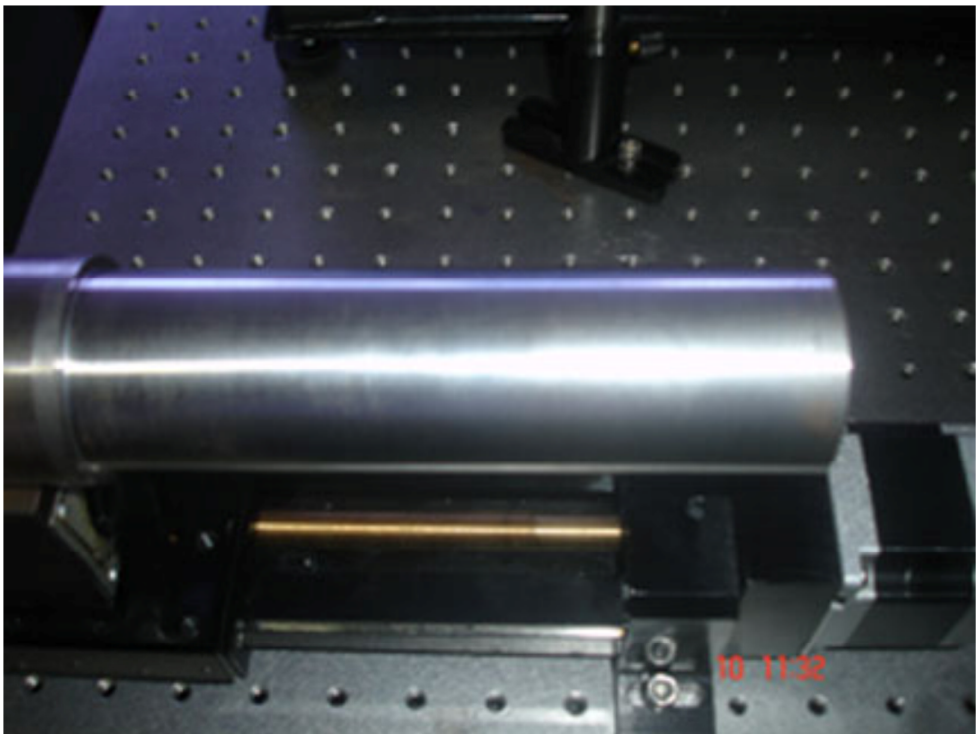

Fig 5.18 Machined surface of the specimen

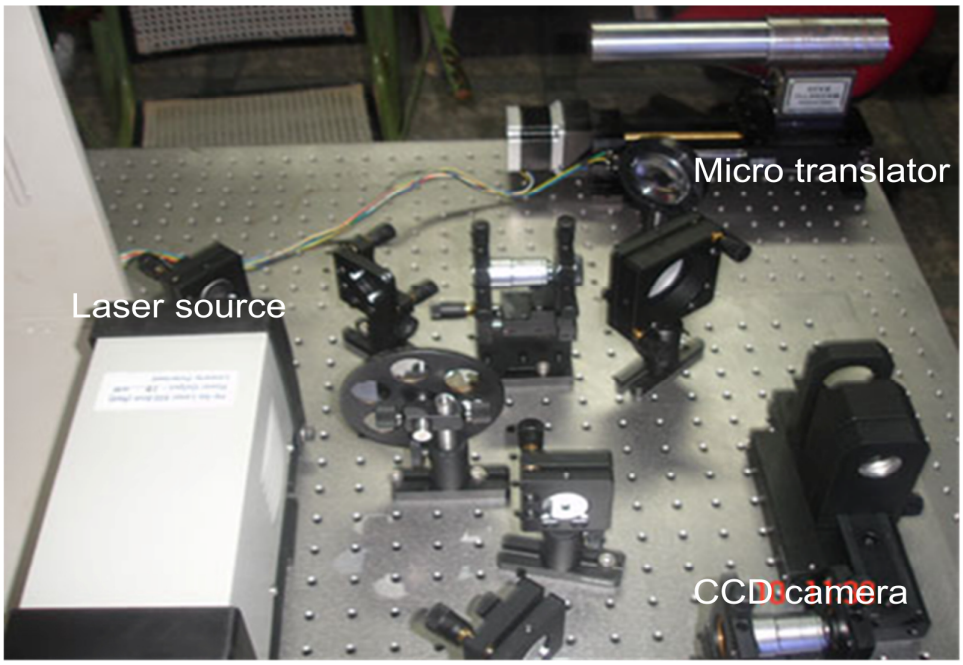

Fig. 5.19 Experimental set up used for speckle image recording

The light distribution on the CCD was viewed through a personal computer. Keeping the laser source position fixed, the machined sample was moved horizontally along its axial direction in short steps with pauses in between using a micro-translator. The test specimen axis and the line of the laser beam were designed to be contained in the same horizontal plane so that effects due to the surface curvature are minimized. The test specimen movement and the capturing of the speckle images are synchronized using Motion Control and NI Vision Development Module software through PCI 6221 DAQ Card. The speckle images of 480 x 640 sizes with 0 to 255 gray levels recorded at a rate of one for each pause of micro translator. They were stored in the personal computer hard disk for later processing. The speckle images of the surface were taken for the entire axial length. The experimental set up used for speckle image recording is shown in Figure 5.19.

5.9.2 Time series construction

The recorded speckle patterns have been statistically analyzed to obtain some significant parameter, which would vary with the surface roughness. It has been already established that the parameters contrast ratio and surface roughness has an inverse relation between them. In the present analysis, the mean gray level value of the histogram of the speckle is taken into consideration as it denotes the intensity of the speckle.

The mean grey level of the histogram is defined as

$$\mu = \frac{\sum_{i=0}^{255} f_i y_i}{\sum_{i=0}^{255} f_i}$$

Where f_i is the number of pixels having y_i gray levels.

The mean gray level values of all the speckle images have been calculated and arranged as per the order of capturing to get a spatial time series for offline analysis. The time series obtained from the sequential speckle images taken over the entire axial length of the test specimen therefore contains this information about chatter-onset and the subsequent chatter-cutting. Using this time series of mean gray level value of the histogram of the speckle, PE is calculated.

For permutation entropy based analysis, the time series is first separated into non overlapping windows of 1024 samples. Normalised PE value is calculated for every window. Variation of PE with respect to moving windows is used for detection of onset of chatter. Here the results of PE of order 6 for a window size of 1024 samples of the time series of the speckle intensity value is presented. These values are found to be the ideal choice for getting optimum speed of calculation with minimum memory restrictions.

Fig. 5.20 shows the variation of PE with respect to length of the work piece (AISI 1025 Carbon Steel) for sudden change in depth of cut from 1 mm to 3 mm. For a length of work piece below 20 mm, it can be observed that there is no significant change in dynamics as indicated by PE values. At 20 mm length of the work piece, a sharp decrease in PE value is observed. This drop in PE indicates increase in regularity of the dynamics thereby indicating the onset of chatter. Above 20 mm PE value fluctuates within a large scale compared to the chatter free region.

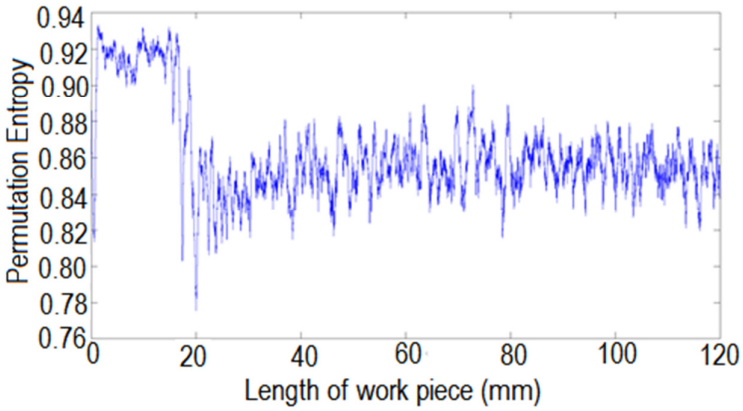

Fig. 5.20 Variation of PE for AISI 1025 Carbon Steel

(speed 360 rpm, feed 0.08 mm/rev)

PE remains almost a constant up to 20 mm length indicating regularity which is indicative of a smooth surface. At 20 mm length, there is a drop in PE value followed by a sudden increase. This is due to a change in the dynamics of the system indicating an increase in roughness. This transition point indicates the onset of chatter is at 20 mm length. This transition in dynamics is verified from the variation in waviness of the surface.

Fig. 5.21 gives the variation of PE for gun metal. PE remains almost a constant up to 19.8 mm length indicating regularity which is indicative of a smooth surface. After 19.8 mm length, there is a drop in PE value followed by a sudden decrease at 54.9. This is due to a change in the dynamics of the system indicating an increase in roughness.

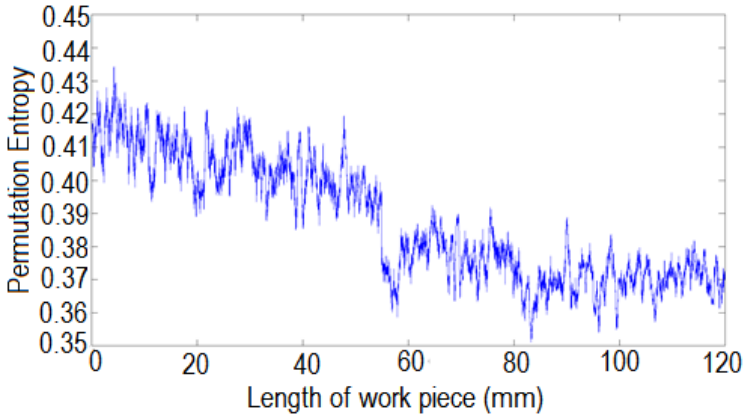

Fig. 5.21 Variation of PE for Gun metal

(speed 360 rpm, feed 0.08 mm/rev)

This transition point indicates the onset of chatter is at 54.9 mm length. This transition in dynamics is verified from the variation in waviness of the surface.

For other materials at various conditions of machining, the PE analysis gives essentially the similar results. It proves that the CRQA methodology is a robust method for the identification of chatter in machining.

5.10 Wilcoxon rank-sum test

The Wilcoxon rank-sum test is a nonparametric test which is based solely on the order in which the observations from the two samples fall by using ranking methods. The Wilcoxon test is valid for data from any distribution, whether normal or not, and is much less sensitive to outliers [115]. It is used for comparing two related samples or repeated measurements on a single sample to assess whether their population mean ranks fluctuate.

Now, to ascertain whether the differences seen in the calculated CRQA variable values is by chance or otherwise, the non parametric Wilcoxon rank-sum test is carried out to find their statistical significance. The test results are given in Table 5.7

Table 5.7 CRQA Variables – Wilcoxon rank-sum test results

Recurrence Variable	Power	Vibration	P (Two tailed)	Significance Level
Percent recurrence	14.218	7.875	0.0004	Highly Significant
Percent determinism	51.208	39.791	0.0002	Highly Significant
Percent laminarity	47.358	13.089	0.0045	Marginally significant
Trap Time	17.149	12.500	0.0130	Significantly different
Entropy	4.557	2.750	0.0003	Highly Significant

The test results show that the difference in values between different sets that can arise by chance is by five per cent or less only in the case of percent recurrence, percent determinism and entropy whereas the remaining three are found to be not highly significant.

5.11 Observations

1) A strong linear relationship among the parameters (feed rate and vibration) and the response (surface roughness) is found using multiple regression

2) The results of the experiments show that the CRQA variable percent determinism, percent recurrence and entropy are sensitive to chatter in cutting.
3) Permutation entropy analysis of the speckle intensity signal establishes the applicability of CRQA methodology in chatter detection in machining.
4) Wilcoxon rank-sum test results show that the difference in values between different sets that can arise by chance is by five per cent or less in the case of percent recurrence, percent determinism and entropy.

5.12 Summary

In this chapter the cross recurrence plot quantification analysis of time series obtained from sensor signals in a machining operation is done based on nonlinear dynamics concepts. The next chapter deals with the conclusions.

6. Conclusion

The focus of the thesis has been to investigate the applicability of CRQA in coupled oscillators to detect couplings and to detect chatter. In the present investigation, experiments are conducted on coupled oscillators and on a lathe. It is found that the CRQA is an effective tool in analysing the non linear dynamics of the coupled systems. By carrying out CRQA analysis on machining signals, point at which the onset of chatter began could be determined. The abrupt changes that are seen in various CRQA variables are suggestive of the onset of chatter.

Linear methods fail to characterize the non linear dynamical systems. It is established that CRQA based methods could bring out salient features of the coupled systems. It is seen that even weak couplings can be characterised by CRQA methods. The surrogate data test shows that the results obtained (Table 4.3) are the true properties of the temporal evolution of the dynamics and contain a degree of deterministic structure. From the Wilcoxon rank-sum test results of the CRQA variables (Table 5.7), it can be inferred that the difference in values between different sets that can arise by chance is by five per cent or less in the case of percent recurrence, percent determinism and entropy. Hence the CRQA variables percent determinism, percent recurrence and entropy are sensitive to chatter in

cutting. Permutation entropy analysis of the speckle intensity signal verifies the fact that CRQA methodology can be used in chatter detection in machining.

It is already established that the metal cutting exhibits low dimensional chaos. The cross recurrence methods can effectively characterize them. The main reason is that the dynamics of most machining processes and systems are nonlinear and CRQA can characterize them adequately. It is possible to extend this technique for online detection of chatter, which can be utilized to control the process. Compared to the conventional chatter detection methods, this method is inexpensive and is a non-contact technique.

In the following section the conclusions of the thesis based on the results obtained are summarised.

6.1 Summary

The conclusions are summarised below:

1. The CRQA analysis reveals nonlinear coupling characteristics that are completely missed by other linear methods.
2. The abrupt changes that are seen in various CRQA variable values are suggestive of the onset of chatter during machining
3. The analysis established that three CRQA variables (Determinism, Entropy and Recurrence rate) are significant variables in characterizing the chatter during machining.
4. Permutation entropy based analysis is utilized to verify the results.

6.2 Benefits

The benefits of the research carried out are as follows:

1. The results obtained by CRQA method are reliable as it is robust against non-stationarity and noise in the signal.
2. Computational time required for estimating the significant variables is lower because feature extraction can be done reliably from even a small size data set. This makes CRP based approaches an effective feature extraction methodology that can be executed for rapid retrieval of information from sensor signals.
3. Coupled oscillator test rig developed has so many parameters that can be varied for an exhaustive study of the non linear systems.
4. CRQA is a universal method that can be applied in various systems for the non linear analysis.

6.3 Contributions

The contributions of the present investigation can be summarised as

1) The set up created for the coupled oscillator test can be utilized for conducting many different experiments in non linear system dynamics characterisation.
2) Development of an efficient approach to detect coupling in coupled systems and chatter in turning
3) Application of cross recurrence concept in machining data

6.4 Future directions

The following are the future directions:

1) The studies may be repeated in complex coupled systems
2) Chatter detection in CNC machine using various sensors.
3) Sensitivity of the significant CRQA variables in high-speed machining.

6.5 Conclusion

The CRQA methodology can be seen as a quantitative decision support system in chatter detection. Any effort made to tackle the issues of noise and stationarity characteristics of sensor signals for signal feature extraction will advance machining principles and practices.

References

1. Katica (Stevanovi´c) Hedrih, Dynamics of coupled systems, Nonlinear Analysis: *Hybrid Systems* 2, 2008, 310–334

2. Alexander Pogromsky and Henk Nijmeijer, Cooperative Oscillatory Behavior of Mutually Coupled Dynamical Systems, *IEEE Transactions on Circuit And Systems—I: Fundamental Theory And Applications*, VOL. 48, NO. 2, 2001, 152-162

3. Kevin Shockley, Matthew Butwill, Joseph P. Zbilut and Charles L. Webber Jr., Cross recurrence quantification of coupled oscillators, *Physics Letters A* 305, 2002, 59–69

4. C.L. Webber Jr. and J.P. Zbilut, Dynamical assessment of physiological systems and states using recurrence plot strategies, *Journal of Applied Physiology* 76 (2) (1994) 965–973.

5. J.P. Zbilut and C.L. Webber Jr., Embeddings and delays as derived from quantification of recurrence plots, *Physics Letters A* 171 (3–4) (1992) 199–203

6. C.L.Webber Jr., J.P. Zbilut, in: A. Colosimo (Ed.), Complexity in the Living: A Modelistic Approach, *Proc. International Meeting, University of Rome La Sapienza*, 1998, p. 101

7. J.P. Zbilut, A. Giuliani, C.L. Webber Jr., Recurrence quantification analysis and principle components in the detection of short complex signals. *Phys. Lett. A* 237, 1998, 131-135

8. Louis M. Pecora and Thomas L. Carroll, Master Stability Functions for Synchronized Coupled Systems, *Physical Review Letters, Volume 80, Number 10*,1998, 2109-2112

9. Satoshi Ito, Minoru Sasaki, Yoji Fujita, Hideo Yuasa, A circularly coupled oscillator system for relative phase regulation and its application to timing control of a multicylinder engine, *Commun Nonlinear Sci Numer Simulat* 15, 2010, 3100–3112

10. Jie Ren, Wen-Xu Wang, Baowen Li and Ying-Cheng Lai, Noise Bridges Dynamical Correlation and Topology in Coupled Oscillator Networks, *Physical Review Letters Prl* 104, 058701, 2010

11. Zaid Odibat, A note on phase synchronization in coupled chaotic fractional order systems, *Nonlinear Analysis: Real World Applications*, 2011, doi: 10.1016/j.nonrwa.2011.08.016

12. S.A. Tobias, Machine Tools Vibrations (VibracionesenMa´ quinas-Herramientas), *URMO*, Spain, 1961.

13. W.W. Seto, Mechanical Vibration Theory and Practice (Teorı´a yProblemas de VibracionesMeca´ nicas), *McGraw-Hill,Panama´* , 1970.

14. F.W. Taylor, On the art of cutting metals, *Transactions of ASME28*, 1907, 31–248404.

15. T. Delio, J. Tlusty and S. Smith, Use of audio signals for chatter detection and control, *ASME Journal of Engineering for Industry 114*, 1992, 145-157.

16. Y. Altintas and P.K. Chan, In-process detection and suppression of chatter in milling, *International Journal of Machine Tools and Manufacture*, Volume 32, 1992, 329-347.

17. Y.S. Tarang and T.C. Li, Detection and suppression of drilling chatter, *International Journal of Dynamic Systems, Measurement and Control,* 116, 1994, 729-734.

18. Bason E. Clancy and Yung C. Shin, A comprehensive chatter prediction model for face turning operation including tool wear effect, *International Journal of Machine Tools & Manufacture* 42, 2002, 1035–1044

19. I. Grabec, J. Gradisek and E. Govekar, A New Method for Chatter Detection in Turning, *Annals of the ClRP* Vol. 48/7/1999

20. X. Q. Li, Y. S. Wong and A. Y. C. Nee, Tool wear and chatter detection using the coherence function of two crossed accelerations, *International Journal of Machine Tools and Manufacture ,Volume 37*, 4, 1997, 425-435

21. Jon R. Pratt and Ali H. Nayfeh, Chatter control and stability analysis of a cantilever boring bar under regenerative cutting conditions, *Phil. Trans. R. Soc. Lond. A* 2001 359, 2001, 759-792

22. M. Xiao, S. Karube, T. Soutome, and K. Sato, Analysis of chatter suppression in vibration cutting, *International Journal of Machine Tools and Manufacture, Volume: 42, Issue: 15,* 2002, Pages: 1677-1685

23. Grzegorz Litak, Chaotic vibrations in a regenerative cutting process, *Chaos, Solitons and Fractals* 13, 2002,153-155

24. Guillem Quintana and Joaquim Ciurana, Chatter in machining processes: A review, *International Journal of Machine Tools and Manufacture*, 2011, doi : 10.1016/ j.ijmachtools.2011.01.001

25. Kong Fansen, Liu Peng and Zhao Xingang, Simulation and Experimental Research on Chatter Suppression Using Chaotic Spindle Speed Variation, *Journal of Manufacturing Science and Engineering, Vol.* 133 / 014502-1, February 2011

26. J.P. Eckmann, S.O. Kamphorst, D. Ruelle, Recurrence Plots of Dynamical Systems, *Europhysics Letters,* 5, 1987, 973–977

27. J.P. Zbilut and C.L. Webber Jr., Embeddings and delays as derived from quantification of recurrence plots, *Physics Letters A* 171 (3–4), 1992, 199–203

28. S. Schinkel, O. Dimigen, and N. Marwan, Selection of recurrence threshold for signal detection, *Eur. Phys. J. Special Topics* 164, 2008, 45–53

29. Matthew B.Kennel, Reggie Brown and Henry D. I. Abarbanel, Determining embedding dimension for phase-space reconstruction using a geometrical construction, *Physical Review A Volume 45, Number 6,* 1992, 3403-3411

30. Joseph P. Zbilut, Alessandro Giuliani and Charles L. Webber, Jr. ,Recurrence quantification analysis and principal components in the detection of short complex signals*, Physics Letters A 237*, 1998, 131- 135

31. J.-P. Eckmann, S.O. Kamphorst, D. Ruelle, Recurrence plots of dynamical systems, *Europhys. Lett. 4,* 1987, 973–979

32. J. P. Zbilut, Power laws, transients, attractors and entropy. In: H. Haken and H.- P. Koepchen, eds., Rhythms in physiological systems. *Springer, Berlin,* 1991, pp. 139–152

33. C.L. Webber Jr. and J.P. Zbilut, Recurrence quantification analysis of nonlinear dynamical systems, Tutorials in contemporary nonlinear methods for the behavioral sciences,(Chapter 2), *M.A. Riley, G. Van Orden, eds*. 2004, pp. 26-94

34. J. P. Zbilut and C. L. Webber, Embeddings and delays as derived from quantification of recurrence plots*, Jr. Phys. Lett. A* 171, 1992, 199-203

35. C.L. Webber and J.P. Zbilut, Dynamical assessment of physiological systems and states using recurrence plot strategies, *J.Appl.Physiol*. 76: 1994, 965-973

36. L.L. Trulla, A. Giuliani, J.P. Zbilut and C.L.Webber Jr., Recurrence quantification analysis of the logistic equation with transients, *Physics Letters A* 223 (4), 1996 255–260

37. M. Zak, J. P. Zbilut, and R. E. Meyers. From instability to intelligence: Complexity and predictability in nonlinear dynamics. *Lecture notes in physics: New series m 49: monographs.* Springer-Verlag, Berlin, 1997

38. P. Faure and H. Korn, A nonrandom dynamic component in the synaptic noise of a central neuron*, Proc. Natl. Acad. Sci. USA* 94, 1997, 650-651

39. A. Giuliani, and C. Manetti, Hidden peculiarities in the potential energy time series of a tripeptide highlighted by a recurrence plot analysis: A molecular dynamics simulation, *Phys Rev E Stat Phys Plasmas Fluids Relat Interdiscip Topics*, 53(6), 1996, 6336–6340

40. F. Orsucci, (Ed.) The Complex Matters of Mind, *World Scientific, Singapore* Vol. 6, 2002, 141-181

41. N. Marwan, J. Kurths: Line structures in recurrence plots, *Physics Letters A*, 336(4–5), 2005, 349–357 DOI:10.1016/j.physleta.2004.12.0

42. T.K. Marcha S.C. Chapmana and R.O. Dendy, Recurrence plot statistics and the effect of embedding, *Physica D* 200, 2005, 171–184

43. S. Schinkel, O. Dimigen, and N. Marwan, Selection of recurrence threshold for signal detection, *Eur. Phys. J. Special Topics* 164, 2008, 45–53

44. Charles L. Webber Jr., Norbert Marwan, Angelo Facchini and Alessandro Giuliani, Simpler methods do it better: Success of Recurrence Quantification Analysis as a general purpose data analysis tool, *Physics Letters A*, 373, 2009, 3753–3756

45. Chiara Mocenni, Angelo Facchini and Antonio Vicino, Comparison of recurrence quantification methods for the analysis of temporal and spatial chaos, *Mathematical and Computer Modelling*, 2010, doi:10.1016/j.mcm.2010.04.008

46. N. Marwan, M. Thiel, and N. R. Nowaczyk, Cross Recurrence Plot Based Synchronization of Time Series, *Nonlinear Processes in Geophysics* 2002, 101–110

47. Joseph P. Zbilut, Alessandro Giuliani and Charles L. Webber, Jr. , Detecting deterministic signals in exceptionally noisy environments using cross-recurrence quantification, *Physics Letters A* 246, 1998, 122- 128

48. Norbert Marwan, and Jürgen Kurths, Nonlinear analysis of bivariate data with cross recurrence plots, *Physics Letters A* 302, 2002, 299–307

49. Rick Dale, Anne S. Warlaumont and Daniel C. Richardson, Nominal cross recurrence as a generalized lag sequential analysis for behavioral streams, *International Journal of Bifurcation and Chaos*, 21, 2010, 1153-1161

50. Eleni I. Vlahogianni, Charles L. Webber Jr., N. Geroliminis and A. Skabardonis, Statistical characteristics of transitional queue conditions in signalized arterials, *Transportation Research Part C* 15, 2007, 392–403

51. S. Bukkapatnam, A. Lakhtakia and S. Kumara, Analysis of sensor signals shows turning on a lathe exhibits low-dimensional chaos, *Physical Review E* 52, 1995, 2375-2387

52. S. Doi and S. Kato, Chatter vibrations of lathe tools, *Transactions of ASME*, 78, 1956, 1127-1134

53. S.A. Tobias, Machine-Tool Vibration, *Blackie and Sons Ltd.: Glasgow, Scotland*, 1965.

54. J. Tlusty and F. Ismail, Basic non-linearity in machining chatter. *CIRP Ann. Manufacturing Technol.* 30, 1981, 299-304

55. I. Grabec, Chaos generated by the cutting process, *Physics Letters A* 117, 1986, 384-386.

56. I. Grabec, Chaotic dynamics of the cutting process, *International Journal of Machine Tools and Manufacture,* 28, 1988, 19–32

57. E. Marui, S. Kato, M. Harashimoto and T. Yamada, The mechanism of chatter vibrations in a spindle work piece system: Part 2 – Characteristics of dynamic cutting force and vibration energy, *ASME Journal of Engineering for Industry* 110, 1988, 242–247

58. J. Warminski, G. Litak, J. Lipski, M. Wiercigroch and M.P. Cartmell, Vibrations in regenerative cutting process synthesis of nonlinear dynamical systems, In: Lavendelis, E. and Zakrzhevsky, M. (eds), *Solid Mechanics and its Applications Vol. 73, Kluver Academic Publishers, Dordrecht,* 2000, pp. 275–283

59. J. Warmi´nski, G. Litak, M.P. Cartmell, R. Khanin and M. Wiercigroch, Approximate analytical solutions for primary chatter in the nonlinear metal cutting model, *International Journal of Sound and Vibration* 259, 2003, 917–933

60. G. Litak, J. Warmi´nski and J. Lipski, Self-excited vibrations in cutting process, In *Proceedings of the 4th Conference on Dynamical Systems – Theory and Applications, Lód´z, Poland*, December 1997, pp. 193–197

61. J.R. Pratt and A.H. Nayfeh, Design and modelling for chatter control, *Nonlinear Dynamics*, 19, 1999, 49–69

62. G. Stepan and T. Kalmar-Nagy, Nonlinear regenerative machine tool vibrations, in: *Proceedings of DETC'97*, Sacramento, California, September 1997

63. D.B. Marghitu, B.O. Ciocirlan and N. Craciunoiu, Dynamics in orthogonal turning process, *Chaos, Solitons & Fractals* 12, 2001, 2343–2352.

64. F.C. Moon and T. Kalmar-Nagy, Nonlinear models for complex dynamics in cutting materials, *Phil. Transansactions of the Royal Society of London* A 359, 2001, 695–711.

65. I.N. Tansel, C. Erkal, T. Keramidas, The chaotic characteristic of three dimensional cutting, *International Journal of Machine Tools and Manufacture*, 32, 1992, 811–827.

66. T. Kalmar-Nagy, J.R. Pratt, M.A. Davies, and M. Kennedy, Experimental and analytical investigation of the subcritical instability in metal cutting. In *Proceedings of the 17th Biennial Conference on Mechanical Vibration and Noise, ASME Design and Technical Conferences, Las Vegas, NV*, September 12-16, 1999.

67. T. Kalmár-Nagy and F. C. Moon, Mode-coupled regenerative machine tool vibrations, *Nonlinear Dynamics of Production Systems, Wiley-VCH, Berlin*, 2004, pp. 129-149

68. P.L.B. Oxley and W.F. Hastings, Predicting the strain rate in the zone of intense shear in which the chip is formed in machining from the dynamic flow stress properties of the work material and the cutting conditions. *Proceedings of the Royal Society of London,* A 356 (1977) 395-410

69. M. Johnson, Nonlinear differential equations with delay as models for vibrations in the machining of metals. *PhD thesis*, Cornell University, 1996

70. M. Johnson and F.C. Moon, Experimental characterization of quasiperiodicity and chaos in a mechanical system with delay, *International Journal of Bifurcurcation and Chaos* 9, 1999, 49-65.

71. H. Abarbanel, Analysis of observed chaotic data, *Springer*, 1996.

72. B. Berger, M. Rokni and I. Minis, The nonlinear dynamics of metal cutting. *International Journal of Engineering Science*, 30, 1992, 1433-1440.

73. B. Berger, I. Minis, Y. Chen, A. Chavali and M. Rokni, Attractor embedding in metal cutting, *International Journal of Sound and Vibration* 184, 1995, 936-942

74. I. Minis and B.S. Berger, Modelling, analysis, and characterization of machining dynamics, *In Dynamics and Chaos in Manufacturing Processes (ed. F. C. Moon), Wiley*, 1998, pp. 125-163.

75. S.T.S. Bukkapatnam, Compact nonlinear signal representation in machine tool operations, In *Proc. 1999 ASME Design Engineering Technical Conference, Las Vegas*, NV, USA, 1999

76. S.T.S. Bukkapatnam, A. Lakhtakia, S. Kumara and G. Satapathy, Characterization of nonlinearity of cutting tool vibrations and chatter. *In ASME Symp. on Intelligent Manufacturing and Material Processing,* vol. 69,1995, pp. 1207-1223.

77. F.C. Moon, Chaotic dynamics and fractals in material removal processes. In *Nonlinearity and chaos in engineering dynamics (ed. J. Thompson & S. Bishop),* Wiley 1994, pp. 250

78. F.C. Moon and H. Abarbanel, Evidence for chaotic dynamics in metal cutting, and classification of chatter in lathe operations. In *Summary Report of a Workshop on Nonlinear Dynamics and Material Processes and Manufacturing (ed. F. C. Moon),* Institute for Mechanics and Materials, 1995, pp. 11-12, 28-29.

79. J. Gradisek, E. Govekar and I. Grabec, Time series analysis in metal cutting: chatter versus chatter-free cutting. *Mech. Sys. Signal Proc.* 12, 1998, 839-854.

80. J. Gradisek, E. Govekar and I. Grabec, Using coarse grained entropy rate to detect chatter in cutting, *Journal of sound and vibration*, 214, 1998, 941-952

81. I. Grabec, J. Gradisek and E. Govekar, A new method for chatter detection in turning. *CIRP Annals.* 48(1), 1999, 29-32.

82. M. Wiercigroch and A.H.D. Cheng, Chaotic and stochastic dynamics of orthogonal metal cutting, *Chaos, Solitons & Fractals* 8, 1997, 715–726.

83. S.A. Tobias and W. Fishwick, The chatter of lathe tools under orthogonal cutting conditions. *Transactions of the ASME* 80, 1958, 1079.

84. J. Tlusty, Analysis of the state of research in cutting dynamics. *CIRP Annals,* 27, 1978, 583-589.

85. H. Poincare, Sur la probleme des trois corps et les équations de la dynamique, *Acta Mathematica* 13, 1890, 1–271

86. M. Small, Applied nonlinear time series analysis, *World Scientific, Singapore,* 2005

87. A. M. Fraser and H. L. Swinney, Independent coordinates for strange attractors from mutual information, *Physical Review A* 33 2, 1986, 1134–1140.

88. M. B. Kennel, R. Brown, and H. D. I. Abarbanel, Determining embedding dimension for phase-space reconstruction using a geometrical construction, *Physics Review A* 45, 1992, 3403.

89. N.H. Packard, J.P. Crutchfield, J.D. Farmer et al., Geometry from a time series, *Physical Review Letters* 45, 1980, 712-716

90. F. Takens, Detecting strange attractors in turbulence, *Dynamical Systems and Turbulence, Warwick, Lecture Notes in Mathematics 898, Springer-Verlag*, 1981, 366-381

91. T. Sauer, J.A. Yorke, and M. Casdagli, Embedology, *Journal of Statistical Physics* 64 1991, 579-616

92. K. Judd and L. Smith, Indistinguishable states-perfect model scenario , *Physica D*, 151, 2001, 224-242

93. J.D. Farmer, E.Ott and J. A Yorke, The dimension of chaotic attractors, *Physica D*, 7 1983, 153-180

94. J. Theiler, Estimating fractal dimension, *Journal of Optical Society of America*, 7 1990, 1055-1073.

95. M. Perc, Introducing nonlinear time series analysis in undergraduate courses, *Fizika A (Zagreb)* 15 (2), 2006, 91–112

96. J.D. Reiss, The analysis of chaotic time series, *Ph.D. thesis, Georgia Institute of Technology*, 2001

97. A. M. Fraser and H. L. Swinney, Independent coordinates for strange attractors from mutual information, *Physical Review A* 33, 1986, 1134-1140

98. R. Shaw, Strange attractors, *Chaotic behavior and information flow. Z. Naturforsch*., 36a, 1981, 80-112.

99. H. Kantz and T. Schreiber, Nonlinear time series analysis, *Cambridge University Press, Cambridge*, 1997.

100. J.P. Eckmann, S.O. Kamphorst, D. Ruelle, Recurrence Plots of Dynamical Systems, *Europhysics Letters,* 5, 1987, 973–977

101. N. Marwan, Encounters With Neighbors - Current developments of concepts based on recurrence plots and their applications, *Ph.D. Thesis, University of Potsdam,* ISBN 3-00-012347-4, 2003

102. N. Marwan, N. Wessel, U. Meyerfeldt, A. Schirdewan and J. Kurths, Recurrence plot based measures of complexity and its application to heart rate variability data, *Physical Review E* 66 (2), 2002, 026702

103. J.P. Zbilut and C.L. Webber Jr., Embeddings and delays as derived from quantification of recurrence plots, *Physics Letters A* 171 (3–4), 1992, 199–203.

104. Norbert Marwan and Jürgen Kurths, Cross recurrence plots and their application, *Mathematical Physics Research at the cutting edge, Nova Science Publishers*, 2004, pp 101-139

105. Kevin Shockley, Cross Recurrence Quantification of Interpersonal Postural Activity, *Journal of Experimental Psychology: Human Perception and Performance,* 2003

106. C.L. Webber Jr., M.A. Schmidt and J.M. Walsh, Influence of isometric loading on biceps EMG dynamics as assessed by linear and nonlinear tools, *Journal of Applied Physiology*, 78, 1995, 814-822.

107. R. Hegger, H. Kantz, L. Matassini, T. Schreiber, Coping with Nonstationarity by Overembedding, *Phys. Rev. Lett.* 84, 2000, 4092

108. Grassberger, P., Schreiber, T. & Schaffrath, C., `Nonlinear time sequence analysis, *Int. J. Bif. Chaos*, 1(3), 1991, pp.521-547

109. KRQA software: http://homepages.luc.edu/~cwebber/

110. J. Gradisek, E. Govekar and I. Grabec, Time series analysis in metal cutting: chatter versus chatter-free cutting. *Mech. Sys. Signal Proc*. 12, 1998, 839-854.

111. J. Gradisek, E. Govekar and I. Grabec, Using coarse grained entropy rate to detect chatter in cutting, *Journal of sound and vibration*, 214, 1998, 941-952

112. I. Grabec, J. Gradisek and E. Govekar, A new method for chatter detection in turning. *CIRP Annals*, 48(1), 1999, 29-32.

113. Bandt C, Pompe B Permutation entropy: a natural complexity measure for time series. *Phys Rev Lett* 88: 174102. doi:10.1103/PhysRevLett.88, 2002, 174102

114. Jacob Elias, V. G. Rajesh, V. N. Narayanan Namboothiri, Recurrence quantification analysis applied to sequential speckle images of machined surface for detection of chatter in turning, *Proc. of SPIE Vol. 7064*, 706408, 2008 0277-786X/08 doi: 10.1117/12.795777

115. Wilcoxon F., Individual Comparisons by Ranking Methods, *Biometrics Bulletin*, 1945, 1 : 80-83